IEEE Access
Multidisciplinary | Rapid Review | Open Access Journal

Received August 25, 2017, accepted October 7, 2017, date of publication October 11, 2017, date of current version February 1, 2018.

Digital Object Identifier 10.1109/ACCESS.2017.2762091

Energy Harvesting Aided Device-to-Device Communication in the Over-Sailing Heterogeneous Two-Tier Downlink

SHRUTI GUPTA, RONG ZHANG, (Member, IEEE), AND LAJOS HANZO, (Fellow, IEEE)
School of Electronics and Computer Science, University of Southampton, Southampton SO17 1BJ, U.K.

Corresponding author: Lajos Hanzo (lh@ecs.soton.ac.uk)

This work was supported in part by EPSRC under Project EP/N004558/1, Project EP/N023862/1, and Project EP/L018659/1, in part by the European Research Council's Advanced Fellow Grant through the Beam-Me-Up Project, and in part by the Royal Society's Wolfson Research Merit Award. The data for the paper can be obtained from the University of Southampton ePrints research repository: 10.5258/SOTON/D0287.

ABSTRACT Device-to-Device (D2D) communication and heterogeneous networks have been considered as promising techniques for alleviating the demand both for increased spectral resources and for additional infrastructure required for meeting the increased tele-traffic. For the sake of improving both the bandwidth efficiency and the network capacity of heterogeneous cellular networks constituted by multiple tiers, a direct D2D communication is arranged between a pair of nearby devices without involving the base station (BS), whilst reusing the cellular resources. We aim for maximising the sum-rate of the energy harvesting (EH) aided D2D links in a two-tier heterogeneous network by superimposing their messages on the downlink resources of mobile users (MUs), which is achieved without unduly degrading MU's throughput. Specifically, our optimization problem relies on the objective function of maximising the D2D sum-rate based on the joint assignment of both the resource blocks (RBs) and of the transmission power for both the EH aided D2D links and the MUs. This non-convex optimization problem, which is intractable in its original form, is then converted to a tractable convex problem, which is then analyzed by invoking the method of Lagrange multipliers of constrained optimization. As a result, an algorithmic solution defined as *joint optimization of RB and power allocation (JORPA)* is proposed, which jointly allocates the RBs and power for the D2D links, whilst relying on the results of Lagrangian constrained optimization, when the base stations (BSs) of different tiers obey one of the following regimes: (a) orthogonal; (b) co-channel; and (c) the proposed co-orthogonal channel deployments. We also propose low complexity heuristic methods for optimizing the D2D transmit power, while defining the D2D-MU matching heuristically and vice versa. The performance of both the JORPA algorithm as well as of the low-complexity heuristic algorithms is quantitatively analyzed using our simulation results for different channel deployments relying on diverse network parameter settings. As expected, orthogonal deployment performs best, followed by the co-orthogonal and co-channel deployments. Moreover, the throughput experienced by the MUs in presence of D2D communication is guaranteed by our co-orthogonal scheme as well as orthogonal scheme, while co-channel suffers a marginal degradation when compared with throughput threshold. We also demonstrate that our *equal power allocation* heuristic method is capable of achieving 96% of the sum-rate achieved by JORPA while other heuristic methods perform less well, implying that the optimization of the D2D-MU matching is indeed crucial for the system considered.

INDEX TERMS Energy harvesting, D2D communication, heterogeneous network, resource reuse, optimization.

I. INTRODUCTION

The evolution of mobile communication networks has always been motivated by the quest for increasing the capacity in order to meet the continuing upsurge of data traffic spurred by the proliferation of wireless services. However, there is limit to the capacity that can be achieved by the current cellular infrastructure. Hence, future cellular wireless networks are expected to accommodate infrastructural

changes for supporting the escalating tele-traffic demands. In order to efficiently exploit both the spectrum as well as the infrastructural investments of mobile network operators, both device-to-device (D2D) communication and heterogeneous networks (HetNets) have been considered as promising techniques for future wireless systems [1].

On one hand, D2D communication enables a pair of mobile users in each other's proximity to establish a direct link for bypassing the base stations, while reusing the spectrum allocated for traditional cellular communication, thereby offloading the backhaul traffic and enhancing the spectral efficiency [2], [3]. On the other hand, in HetNets, various low-power micro-, pico- and femto-BSs are distributed across the traditional macro cell network for improving both the coverage and capacity of conventional systems [4]. Hence, it is natural to amalgamate the benefits of both techniques in order to achieve an increased design flexibility. However, D2D communication underlaying HetNets will bring about many new challenges, including sophisticated interference management due to the co-existence of different traffic patterns, different spectral bands and diverse user densities in the network etc. Hence, recent research activities have been devoted to investigating the potential of D2D-based heterogeneous networks [5]–[8].

Along with spectral efficiency, another key design objective in future wireless networks is the improvement of energy efficiency, especially that of battery-powered wireless devices. For optimising the device's operation and prolonging the lifetime of devices and networks, energy harvesting (EH) technology is widely considered as an appealing solution that can scavenge energy from the ambient energy resources (e.g. solar, wind, thermal, RF energy etc.) [9]. This energy harvesting process results in the random arrival of energy, and hence the devices have to store this energy to be used later [10]. Hence, different EH network models have been investigated, ranging from point to point communication [11]–[13], to cooperative networks [14]–[19] and to heterogeneous networks [20]–[22].

Specifically, Yang and Ulukus [11] as well as Tutuncuoglu and Yener [12] conceived optimal policies for minimising the transmission completion time, where a transmitter node having either an idealized infinite or a realistic finite storage capacity, harvest energy. He *et al.* [13] introduced geometric water filling for their power allocation problem with the objective of maximizing the data rate as well as minimizing the transmission completion time of the EH aided communication. In the context of cooperative communication, Medepally and Mehta [14] investigated a system that uses energy harvesting relays, where it is observed that the energy usage at the relay node and its availability for relaying depends not only on the energy harvesting rate, but also on the transmit power settings as well as on the total number of relay nodes in the system. On the other hand in Ahmed *et al.* [15] considered optimal power allocation both for a conventional and for a buffer aided link-adaptive energy harvesting relay-aided system. In our previous work of [16], we considered a diamond-topology relay network, where the EH source and the EH-aided relay nodes invoke a successive relaying scheme in conjunction with finite buffers for maximising the system throughput. In [23], Tutuncuoglu *et al.* derived the optimal achievable rates for an EH system in the context of two-way relaying employing sophisticated relaying strategies, while in [18], Ding *et al.* investigated the outage performance of different power allocation strategies, in which multiple source-destination pairs communicate via EH-aided relays. Roseveare and Natrajan [19] formulated a new algorithm for constrained utility maximisation problems encountered in a cooperative network of wireless sensor nodes. By contrast, Zhu *et al.* [20] derived the average harvested energy as well as the uplink rate of a massive MIMO-assisted HetNet. The joint optimization of user association and energy allocation was invoked for minimizing the power-grid-assisted energy consumption in HetNet [21]. Finally, Ghazanfari *et al.* [22] provided an overview of RF based ambient energy harvesting demonstrating the potential trade-offs in ultra-dense small cell networks.

However, the research of HetNets incorporating EH aided underlay D2D links, is still in its infancy, despite the promising early studies [24]. Yang *et. al.* [24] considered a HetNet environment, where the energy is harvested from the access points by the mobile users which can also act as relays once they have stored sufficient harvested energy. These mobile relays then utilise their harvested energy in D2D transmission mode for relaying the downlink transmission from access points. Specifically, Yang *et. al.* [24], investigated the effects of energy harvesting related parameters, as well as those of for the access point density and of the user density on the outage probability.

Against the above background, we consider a two-tier HetNet supporting multiple MUs that are associated either with macro-BS (MBS) or with pico-BSs (PBSs) under various spectrum sharing arrangements as well as multiple underlaying D2D links relying on energy harvesting and reusing the downlink cellular resources for their communication. At the current state-of-the-art, most existing contributions advocate uplink resource reuse for the D2D links [25]–[28]. However, when the D2D links are close to the BS, the near-far effects may impose strong interference on the MU's transmission. Despite this limitation, there is a paucity of contributions on downlink resource reuse at the D2D links, even though this is also important, especially, because it also reflects the worst case interference scenario. Hence this problem is considered in our treatise.[1] Our resource allocation is formulated as an optimization problem maximizing the D2D sum-rate, which is achieved by invoking the joint optimization of the D2D-MU matching, and the power allocation of both the D2D links as well as of the MUs, without violating the throughput constraints of the MUs and without exceeding the power budget

[1]The methodologies developed in this work can be readily extended to uplink resource reuse scenarios by simply considering the throughput guarantee at the BS.

constraints as well as the EH constraints of the D2D links. There are typically two types of spectrum sharing strategies among the BSs of different tiers in HetNets, namely orthogonal spectrum sharing and co-channel spectrum sharing. In this paper, we also propose a spectrum sharing strategy, termed as *Co-orthogonal spectrum sharing*, which subsumes both of the above arrangements. The major contributions of this treatise are as follows:

- Co-orthogonal spectrum sharing: In the proposed arrangement, N sub-channels are shared amongst the MBS and PBSs, while the remaining $(M - N)$ channels are orthogonally shared among the MBS and PBSs. This means that for N sub-channels, the system operates in co-channel deployment, while for the remaining $(M-N)$ channels, the system operates in orthogonal deployment. This arrangement reduces the interference imposed, when compared to the classic co-channel deployment associated with $N = M$ and improves the spectrum exploitation of orthogonal deployment having $N = 0$.
- The sum-rate maximization problem of energy harvesting D2D links reusing the downlink resources of a two-tier HetNet is formulated as a mixed integer non-linear program, which is transformed into a more tractable form and its solution is obtained using the classic Lagrangian method of multipliers.
- Based on the theoretical analysis of the optimization problem, we proposed an algorithmic solution termed as the *Joint Optimization of Resource Block and Power Allocation(JORPA)* for D2D links.
- We also propose the following heuristic methods:
  1) *Equal Power Allocation (EPA):* In this method, the power consumption of the D2D links relies on the harvesting and dissipation strategy associated with equally sharing the power over all the reused RBs, while using optimal D2D-MU matching.
  2) *Random D2D-MU Matching (RM):* In this method, the D2D-MU matching is random, while the power consumption is optimized based on the EH and the maximum power budget constraints.
  3) *Maximum Distance D2D-MU Matching (MDM):* In this method, D2D-MU matching is based on the maximum distance between the D2D link and MU, while the power consumption is optimized under the EH and on the maximum power budget constraints.
- The proposed JORPA algorithm and the heuristic methods were analysed in the context of different parametric settings. Our performance results reveal that the proposed heuristic EPA method is capable of achieving approximately 96% of the sum-rate attained by our JORPA algorithm at a much lower complexity, while our other two heuristic methods perform less well compared to the JORPA solution, indicating that the D2D-MU matching parameters constitute a more crucial set of variables in our problem formulation. Hence, we have to achieve optimized D2D-MU matching, while the power can be heuristically assigned.
- The impact of the presence of D2D communication in two-tier HetNet was evaluated in terms of the MU's throughput associated with either the MBS or the PBSs. Our proposed co-orthogonal scheme is capable of achieving 50% higher than the required throughput of MUs associated with the MBS while 24% higher than that required by the MUs served by the PBSs.

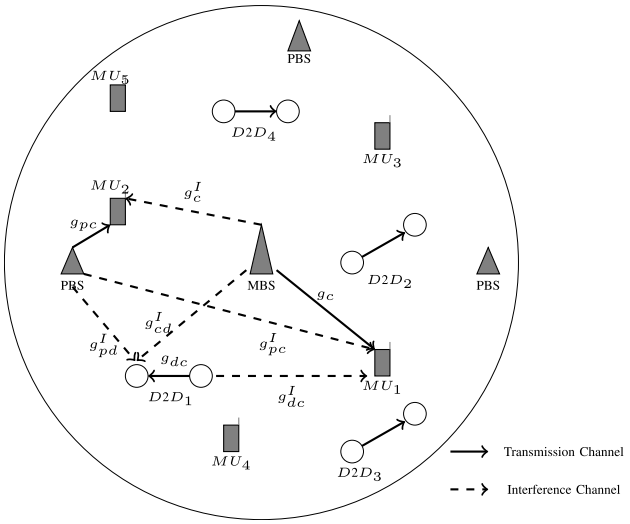

FIGURE 1. An illustration of the relevant transmission and interference patterns in our heterogeneous cellular network, when HetNet supports co-channel spectrum sharing. The D2D links share the MU's downlink resources for their transmission. Here the $D2D_1$ link reuses the RB of MU_1 associated with the MBS, hence this D2D link imposes interference on the MUs communicating within the same RB (MU_2) operating under co-channel deployment, as depicted in the figure. Also other D2D links and MUs will have similar interference patterns depending on their spectrum sharing, however it is not highlighted in the figure for clarity.

To the best of our knowledge, the optimization and analysis of EH aided D2D communication in the downlink of HetNets is a relatively unexplored research area in the context of both the radio resource and power allocation of the D2D links as well as of the MUs. Hence exploring this interesting area is the motivation behind this work.

The rest of the paper is organized as follows. In Section II, our system model is presented, followed by the formulation of the optimization problem. The optimization problem is then analysed and an algorithmic solution relying on the Lagrangian method of multipliers is proposed in Section III, followed by our heuristic methods in Section IV. The proposed algorithms are then quantitatively analysed and discussed in Section V. Finally we conclude this treatise in Section VI.

II. THE HETEROGENEOUS DOWNLINK MODEL AND PROBLEM FORMULATION

We consider a hybrid single cell environment comprising a macro-BS (MBS) covering a cell of radius R overlaid by P randomly located pico-BSs (PBSs). In this HetNet setting, there are D energy harvesting D2D links reusing the downlink (DL) resources of C MUs, as shown in Fig. 1. The

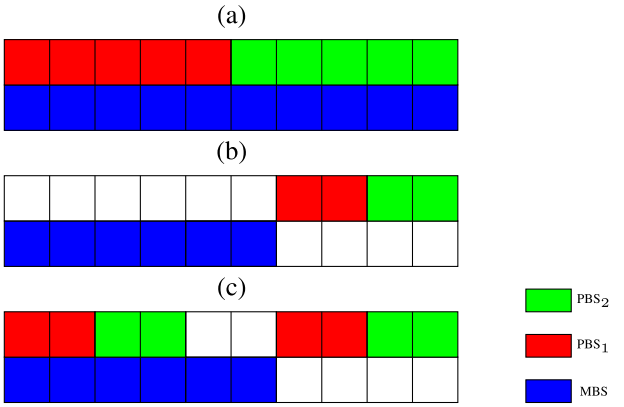

FIGURE 2. An illustration of the different spectrum sharing regimes when there are M sub-channels for distribution among the single MBS and P PBSs with $M = 10$, $N = 4$ and $P = 2$. Note that equal sharing among PBSs is just an example fpr explaining the spectrum sharing schemes, while the allocation of sub-channels is dependent on the traffic load of the PBSs. (a) Co-channel Spectrum sharing. (b) Orthogonal Spectrum sharing. (c) Co-orthogonal Spectrum sharing.

power budget of the MBS is denoted by P_C^{max}, while that of each PBS is P_P^{max}, where the DL transmit power allocated for each MU associated with either the MBS or one of the PBSs is obtained through optimization, as described later in this section. We assume that the DL transmission of each BS activates all of its allocated sub-channels all the time. The two well-known spectrum sharing schemes that have been richly documented in the literature [29] are described below along with our proposed strategy:

1) *Co-Channel Spectrum Sharing:* Each tier transmits on all the sub-channels of Fig. 2(a). In this figure, the MBS and PBSs share a pool of M DL channels, where each of the P PBSs has $\frac{M}{P}$ orthogonal sub-channels. Hence, the MUs DL reception associated with the MBS is contaminated by one of the PBSs transmitting in the DL to the MUs associated with it, while all the PBSs DL transmissions suffer from the interference inflicted by the MBS's DL transmission on all the channels. Moreover, the D2D communications reusing the DL RBs of the MUs experience interference both from the MBS and PBSs present in the system. For example, if we have $P = 2$ PBSs and $M = 10$ sub-channels, then these 10 sub-channels are used for the co-channel sub-band. Thus, the MBS will use all 10 sub-channels and each of the $P = 2$ PBSs will use 5 sub-channels orthogonally in this co-channel sub-band, as shown in Fig. 2(a).
2) *Orthogonal Spectrum Sharing:* Both the MBS and the PBSs are allocated a dedicated set of sub-channels, which are orthogonal to each other. If there are M channels, then the set of PBSs is exclusively supported by N sub-channels, while the remaining $(M - N)$ sub-channels are allocated to the MBS. Then each PBS is allocated a dedicated set of orthogonal sub-channels by partitioning the N sub-channels among P PBSs, as shown in Fig. 2(b). This arrangement reduces the co-channel interference imposed by the MBS and PBSs on the D2D links, which is achieved at the expense of granting only a reduced bandwidth for each MBS and PBSs. For example, if we have $P = 2$ PBSs, $M = 10$ and $N = 4$ sub-channels, then these 4 sub-channels are earmarked for pool of PBSs for orthogonal deployment. Thus, the MBS will use remaining 6 sub-channels and each of the $P = 2$ PBSs will use 2 sub-channels orthogonally.
3) *Co-orthogonal spectrum sharing:* The proposed strategy is a unification of the pair of richly investigated channel allocation strategies mentioned above. In our hybrid deployment, M sub-channels are allocated for ensuring that N sub-channels are used by the MBS and by all the PBSs in a co-channel interfering fashion, while the remaining $(M - N)$ sub-channels are orthogonally distributed among the MBS and PBSs in the system. This is shown in Fig. 2(c).[2] Thus, this channel allocation deployment caters for a reduced interference at the D2D links, when it reuses the RBs of MUs served in orthogonal spectrum sharing, while it efficiently exploits the bandwidth at each BS by relying on co-channel deployment as well. For example, if we have $P = 2$ PBSs, $M = 10$ and $N = 4$ sub-channels, then these 4 sub-channels are used for the co-channel sub-band, while the remaining 6 are earmarked for orthogonal reuse. Thus, the MBS will use all 4 sub-channels and each of the $P = 2$ PBSs will use 2 sub-channels orthogonally in this co-channel sub-band. Furthermore, from the orthogonal set of sub-bands, each of the BSs will use 2 additional sub-channels, which are orthogonally distributed between the two tiers.

In case of our co-orthogonal sharing, the D2D links can reuse any of the sub-bands and for the sake of intelligently reducing the interference experienced by the D2D links, we invoke an interference-threshold I_{Th} for the D2D link. The threshold is used in order to decide, whether the D2D link should reuse the RB of the MUs served by an orthogonal sub-band or whether it should opt for using a co-channel sub-band. When implementing this flexible spectrum sharing scheme, we denote the total interference imposed on the d^{th} D2D link by all the BSs as $I_d, \forall d \in D$. If the total interference at the d^{th} D2D link is higher than the threshold I_{Th} ($I_d \geq I_{Th}$), then the d^{th} D2D link reuses the RBs of those specific MUs that are served by the orthogonal spectral sub-band allocated to their serving BSs. Otherwise it reuses that the RBs of the MUs served by the co-channel sub-band allocated by their serving BSs. This is clearly depicted in Fig. 3, where the interference experienced by the d^{th} D2D links from the DL

[2]Note that our co-orthogonal scheme is different from soft frequency reuse (SFR) scheme because SFR is an inter-cell interference management scheme that depends on physical location of MUs for the allocation of frequency reuse, while the proposed co-orthogonal scheme is also an interference management scheme, however it does not depend on explicit physical restriction of D2D links.

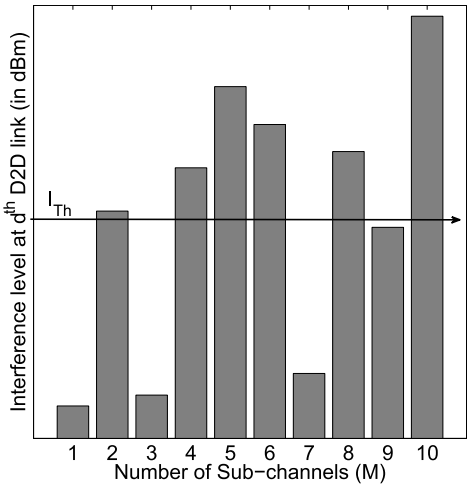

FIGURE 3. Interference experienced by the d^{th} D2D link on each of the M sub-channels distributed amongst MBS and PBSs. Here M=10 sub-channels, N=4 sub-channels, P=2 PBSs.

transmission of both the MBS and PBSs is shown for all the M sub-channels available for the DL transmission of MUs. It can be seen in Fig. 3 that the d^{th} D2D link experiences interference below the threshold I_{Th} on the sub-channels 1, 3, 7 and 9 indicating that when these sub-channels are reused at the d^{th} D2D link, it opts for using a co-channel sub-band, while on all other sub-channels it reuses an orthogonal sub-band. This interference-based switching is introduced for the reduction of the overall interference on the D2D links, which is comprised of that emanating from the MBS and/or PBS depending on the spectrum sharing scheme adopted. On the other hand, the MUs are randomly associated with the orthogonal or co-channel sub-bands available at their associated BSs. Furthermore, if we have $I_{Th} = 0$dBm, then all the D2D links will aim for reusing the co-channel sub-band, resulting in a co-channel spectrum sharing scenario. By contrast, for $I_{Th} >= (P_C^{max} + P_p^{max})$ the system relies on orthogonal spectrum sharing and for $I_{Th} \in (0, \{P_C^{max} + P_p^{max}\})$ it defines the proposed co-orthogonal spectrum sharing scenario.

We study the downlink and assume that each MU can be served by only a single BS. This MU-BS association ($x_c \in \{0, 1\}$) is defined on the basis of signal strength experienced by the MU from all the BSs. Each MU is associated with the specific BS that provides the maximum received signal power to the MU. If the signal strength received at c^{th} MU from the MBS is higher than that received from the PBSs, this MU is served by the MBS ($x_c = 1$), otherwise it is served by the PBSs ($x_c = 0$). Moreover, since the power budget of the MBS is higher than that of the PBS, we introduce biasing at PBSs in order to support traffic offloading from the MBS to the PBSs. This in turn means that for calculating the signal strength from the PBSs, we will take into account the biasing factor B for the MU's association. For the sake of convenient exposition, we define another binary parameter $x_{pc} \in \{0, 1\}$, which denotes the association of the MUs with their respective PBSs, implying that $x_{pc} = 1$ if MU c is associated with the p^{th} PBS and 0 otherwise. Each MU is served by a single dedicated downlink RB obtained from the pool of sub-channels allocated to its associated BS and it is assumed that each MU's downlink RB can be reused by only a single D2D link.[3] This constitutes a one-to-many mapping, where a single D2D link can be mapped to multiple RBs of different MUs [30], [31]. Let $y_{dc} \in \{0, 1\}$ represent the D2D-MU matching. Then, if the RB of the c^{th} MU is reused by the D2D link d, we have $y_{dc} = 1$, otherwise y_{dc} is set to zero. Hence, for the sake of satisfying this assumption, we have $\sum_{d=1}^{D} y_{dc} = 1 \; \forall \; c$. Moreover, for the co-channel spectrum sharing scenario we also have an additional constraint that prevents the D2D links from reusing the same RB of different MUs that are served by BSs of different tiers and are in a co-channel scenario with each other, as facilitated by $\sum_{c \in C_{co}} \sum_{d=1}^{D} y_{dc} = 1$.[4]

We also assume to have an energy harvesting capability at the D2D transmitter (TX), and as a consequence, the energy causality constraint is imposed on the transmit power of the D2D link, which implies that during the communication process, the device's total energy expenditure should not exceed its total energy harvested upto that time instant. The amount of energy harvested at the time instant t_i is denoted as $E_{d,i}$ units for $i \in [0, K-1]$, where the harvesting process starts at $t_0 = 0$ and its deadline is $t_K = T$. We define an *epoch* as the time interval between two consecutive energy arrival events, whose length is defined as $\tau_i = (t_i - t_{i-1})$. We stipulate the idealised simplifying assumption that the transmitter knows both the arrival instant and the amount of energy non-causally, i.e. in advance. Throughout this treatise, all the channels in the network obey independent and identical Rayleigh distribution. We define g_c (or g_{pc}) as the transmission channel gain between the MBS (or p^{th} PBS) and c^{th} MU. Similarly, g_{dc} represents the gain of the channel traversing from the D2D TX to the receiver (RX) of the d^{th} D2D link reusing the RB of MU c. Furthermore, the interference channel's gain spanning from the MBS (or p^{th} PBS) to the d^{th} D2D link on the c^{th} MU's RB is denoted by g_{cd}^I (or g_{pd}^I). Similarly, g_{dc}^I represents the gain of the interference channel spanning from the D2D link d to the c^{th} MU. Based on the channel allocations at the BS as well as MU-BS association, we define g_c^I and g_{pc}^I as another set of interference channel gains of the links spanning from the MBS to the MUs associated with the PBSs and that from the p^{th} PBS to the MUs associated with the MBS, respectively. Fig. 1 clearly illustrates all the above-mentioned channels gains.

For an energy arrival instant t_i, the d^{th} D2D link's data rate can be expressed in Eq. (1) (given at top of next page),[5] where $P_{dc,i} \geq 0$ denotes the transmit power of the d^{th}

[3]Note there might exists a scenario where the PBSs might be allocated a large number of RBs, which restricts the interference margin for D2D links resulting in lower D2D sum-rate, however our optimization algorithm presented in this treatise will be still applicable in this rare scenario.

[4]C_{co} refers to the set of MUs served on the downlink RB in co-channel by their respective BSs.

[5]Here $y_{dc,i}$ refers to D2D-MU matching for the i^{th} epoch of EH.

$$r_{d,i} = \sum_{c=1}^{C} y_{dc,i} \log_2 \left(1 + \frac{P_{dc,i} g_{dc}}{(\beta_c x_c + (1-\beta_c)) P_c g^I_{cd} + \sum_{p=1}^{P} (1-\beta_c x_c) x_{pc} P_p g^I_{pd}) + N_0}\right) \forall i, d \quad (1)$$

D2D link on the c^{th} MU's RB at time instant t_i, which is constrained by our energy causality as well as power budget, while $P_c \geq 0$ and $P_p \geq 0$ are the allocated transmit power of the MBS and that of the p^{th} PBS to the associated MU c under their power budgets, respectively, while N_0 is the noise power density. Furthermore, β_c denotes the spectrum sharing strategy employed by the BS in the downlink for the c^{th} MU, where $\beta_c = 1$ represents perfect orthogonality while $\beta_c = 0$ corresponds to co-channel spectrum sharing.

Since the existing cellular communication is complemented by D2D communication for the sake of improving both the bandwidth efficiency and network capacity, the MUs have a higher priority than the D2D links. Thus, we introduce a QoS target for each MU associated with the MBS or PBSs in terms of their minimum required throughput of R_c or R_p, respectively, for preventing the undue degradation of the cellular communication,

$$\sum_{d=1}^{D} y_{dc,i} x_c \log_2 \times \left(1 + \frac{P_c g_c}{N_0 + g^I_{dc} P_{dc,i} + (1-\beta_c x_c) I_P}\right) \geq R_c \quad \forall i, c \quad (2)$$

and

$$\sum_{d=1}^{D} y_{dc,i}(1-x_c) \log_2 \left(1 + \frac{\sum_{p=1}^{P} x_{pc} P_p g_{pc}}{N_0 + g^I_{dc} P_{dc,i} + (\beta_c x_c + (1-\beta_c)) I_M}\right) \geq R_p \quad \forall i, c \quad (3)$$

where $I_P = \sum_{p=1}^{P} x_{pc} p^I_p g^I_{pc}$ is the interference arriving from the active PBSs, while $I_M = p^I_c g^I_c$ is the interference emanating from the MBS that is active, when the system operates either in co-channel or co-orthogonal spectrum sharing environments. Note that the transmit power of the serving PBSs is formulated as a summation for ensuring that the expression accounts for the power of the p^{th} transmitting PBS for the c^{th} MU, since x_p would be 1 only for the transmitting PBS and 0 for others.

We aim to maximize the sum-rate of EH aided D2D links achieved by the deadline of T, while satisfying the energy causality constraints at the D2D links as well as meeting the throughput constraints of the cellular communication by appropriately matching each D2D link with the MU for resource reuse and assigning the optimal power for both the D2D transmission and for the downlink transmission of MUs associated with the BSs under their respective power budgets. Explicitly, this resource allocation problem can be formally stated as an optimization over $\boldsymbol{y_{dc}}, \boldsymbol{P_{dc}}, \boldsymbol{P_c}$ and $\boldsymbol{P_p}$[6]:

$$\underset{\{\mathbf{y_{dc}}, \mathbf{P_{dc}}, \mathbf{P_c}, \mathbf{P_p}\}}{\text{maximize}} : \sum_{i=1}^{K} \sum_{d=1}^{D} r_{d,i} \quad (4a)$$

subject to:

$$\sum_{d=1}^{D} y_{dc,i} \leq 1 \quad \forall i \in K,\ c \in C; \quad (4b)$$

$$\sum_{c \in C_{co}} \sum_{d=1}^{D} (1-\beta_c) y_{dc,i} \leq 1 \quad \forall i \in K; \quad (4c)$$

$$\sum_{c=1}^{C} y_{dc,i} P_{dc,i} \leq P_D^{max} \quad \forall i \in K,\ d \in D; \quad (4d)$$

$$\sum_{\kappa=1}^{i} \sum_{c=1}^{C} y_{dc,\kappa} P_{dc,\kappa} \tau_\kappa \leq \sum_{\kappa=0}^{i-1} E_{d,\kappa} \quad \forall i \in K, d \in D; \quad (4e)$$

$$\sum_{c=1}^{C} (1-x_c) x_p P_p \leq P_P^{max} \quad \forall i \in K, \forall p \in P; \quad (4f)$$

$$\sum_{c=1}^{C} x_c P_c \leq P_C^{max} \quad \forall i \in K; \quad (4g)$$

$$\sum_{d=1}^{D} y_{dc,i} x_c \log_2 \times \left(1 + \frac{P_c g_c}{N_0 + g^I_{dc} P_{dc,i} + (1-\beta_c x_c) I_P}\right) \geq R_c \quad \forall i \in K, \quad c \in C; \quad (4h)$$

$$\sum_{d=1}^{D} y_{dc,i}(1-x_c) \times \log_2 \times \left(1 + \frac{\sum_{p=1}^{P} x_{pc} P_p g_{pc}}{N_0 + g^I_{dc} P_{dc,i} + (\beta_c x_c + (1-\beta_c)) I_M}\right) \geq R_p \quad (4i)$$

$$\forall i \in K, \quad c \in C;$$

$$y_{dc,i} \in \{0,1\}; \quad P_{dc,i} \geq 0;$$

$$P_c \geq 0; \quad P_p \geq 0 \ \forall i \in K,\ c \in C,\ d \in D. \quad (4j)$$

where the objective function (OF) of Eq. (4a) is a non-convex function. Eq. (4b) represents the constraint imposed on the D2D-MU matching, which implies that each RB of MU can only be reused by at most one D2D link. By contrast, in case of co-channel spectrum sharing we have an additional constraint in terms of D2D-MU matching given by Eq. (4c) that avoids the multiple reuse of the same RB by D2D links. The power budget constraint of each D2D link d reusing the cellular RBs is stated by Eq. (4d), while the amount of energy consumed by each D2D link's transmission is constrained by the amount of energy harvested, as demonstrated in Eq. (4e). Furthermore, the MBS and PBSs maintain reliable connections with their associated MUs under the power budget P_C^{max} and P_P^{max} given in Eq. (4g) and Eq. (4f) respectively. This is followed by the throughput constraints of the MUs associated with either the MBS or with one of the P PBSs,

[6]Bold letters represent vectors

as formulated in Eq. (4h) and Eq. (4i), respectively. Finally, Eq. (4j) represent the feasibility constraints.

III. JOINT OPTIMIZATION OF RESOURCE BLOCK AND POWER ALLOCATION FOR D2D LINKS

Since the OF and the throughput constraints in Eq. (4) are non-convex and the variables are either binary or continuous, we are faced with a non-convex mixed integer non-linear programming problem, which is a challenging one in its original form. In this section, we will first transform the problem of Eq. (4) to a more tractable form according to Proposition 1, followed by the analysis of this problem.

Proposition 1: The problem of Eq. (4) is equivalent to the following optimization problem:

$$\underset{\{\mathbf{y_{dc}},\mathbf{p_{dc}}\}}{\text{maximize}} \ \sum\nolimits_{i=1}^{K}\sum\nolimits_{d=1}^{D}\tilde{r}_{d,i} \tag{5a}$$

subject to:

$$\sum\nolimits_{d=1}^{D} y_{dc,i} \le 1 \quad \forall i \in K,\ c \in C; \tag{5b}$$

$$\sum\nolimits_{c\in C_{co}}\sum\nolimits_{d=1}^{D}(1-\beta_c)y_{dc,i} \le 1 \quad \forall i \in K; \tag{5c}$$

$$\sum\nolimits_{c=1}^{C} y_{dc,i}P_{dc,i} \le P_D^{max} \quad \forall i \in K,\ d \in D; \tag{5d}$$

$$\sum\nolimits_{\kappa=1}^{i}\sum\nolimits_{c=1}^{C} y_{dc,\kappa}P_{dc,\kappa}\tau_\kappa \le \sum\nolimits_{\kappa=0}^{i-1} E_{d,\kappa} \quad \forall i \in K,\quad d \in D; \tag{5e}$$

$$\sum\nolimits_{d=1}^{D}\sum\nolimits_{c=1}^{C}(1-x_c)x_{pc}\frac{\alpha_p}{g_{pc}}y_{dc,i}P_{dc,i}g^I_{dc} \le P_P^{max} \tag{5f}$$

$$-\sum_{c=1}^{C}(1-x_c)x_{pc}\frac{\alpha_p}{g_{pc}}[(\beta_c x_c+(1-\beta_c))I_M+N_0]$$
$$\forall i \in K,\quad p \in P;$$

$$\sum\nolimits_{d=1}^{D}\sum\nolimits_{c=1}^{C} x_c\frac{\alpha_c}{g_c}y_{dc,i}P_{dc,i}g^I_{dc} \le P_C^{max} \tag{5g}$$

$$-\sum_{c=1}^{C} x_c\frac{\alpha_c}{g_c}[(1-\beta_c x_c)I_P+N_0] \quad \forall i \in K;$$
$$y_{dc,i} \in \{0,1\};\quad P_{dc,i} \ge 0;\ \forall i \in K,\ c \in C,\ d \in D. \tag{5h}$$

where $\alpha_c = 2^{R_c}-1$, $\alpha_p = 2^{R_p}-1$ and,

$$\tilde{r}_{d,i} = \sum_{c=1}^{C} y_{dc,i}\log_2\left(1+\frac{g_{dc}P_{dc,i}}{e_{dc}N_0+f_{dc}P_{dc,i}+I_{dc}}\right),$$

$$e_{dc} = 1+(\beta_c x_c+(1-\beta_c))\frac{\alpha_c}{g_c}g^I_{cd} + (1-\beta_c x_c)\sum_{p=1}^{P}\frac{x_{pc}\alpha_p g^I_{pd}}{g_{pc}} \quad \forall d \in D,\ c \in C;$$

$$f_{dc} = (\beta_c x_c+(1-\beta_c))\frac{\alpha_c}{g_c}g^I_{cd}g^I_{dc} + (1-\beta_c x_c)\sum_{p=1}^{P}\frac{x_{pc}\alpha_p g^I_{pd}}{g_{pc}}g^I_{dc} \quad \forall d \in D,\ c \in C;$$

$$I_{dc} = (1-\beta_c)\left[\frac{\alpha_c}{g_c}g^I_{cd}I_P+\sum_{p=1}^{P}\frac{x_{pc}\alpha_p g^I_{pd}}{g_{pc}}I_M\right] \quad \forall d \in D,\quad c \in C. \tag{6}$$

Proof: Refer to Appendix A for the proof. □

Note that the optimization variables have been reduced to $\{\mathbf{y_{dc}}, \mathbf{P_{dc}}\}\forall d \in D, c \in C$ in the equivalent problem of Eq. (5). Consequently, the feasibility of Eq. (4) is now explicitly revealed by Eq. (5f) and Eq. (5g), which implies that the interference power generated by the D2D links should not exceed the remaining power of the BSs. Although the problem is still a mixed integer non-linear problem, it is more readily solvable in this form, which we will see by first investigating the convexity of the transformed problem of Eq. (5) in Lemma 1.

Lemma 1: The equivalent maximization problem in Eq. (5) preserves convexity with respect to the variables $\{\mathbf{y_{dc}}, \mathbf{P_{dc}}\}\forall d \in D, c \in C$.

Proof: Let us re-write the equivalent rate for the D2D link of Eq. (6), $\tilde{r}_{d,i}$ as:

$$\tilde{r}_{d,i} = \sum\nolimits_{c=1}^{C} y_{dc,i}\log_2[1+w(P_{dc,i})],$$

where $w(P_{dc,i}) = \frac{g_{dc}P_{dc,i}}{e_{dc}N_0+f_{dc}P_{dc,i}+I_{dc}}$. By evaluating the second order derivative of $\tilde{r}_{d,i}$, we get

$$\tilde{r}''_{d,i} = \frac{w''(P_{dc,i})[1+w(P_{dc,i}))]-[(w'(P_{dc,i}))^2]}{\ln(2)[1+w(P_{dc,i})]^2}, \tag{7}$$

where we have $w''(P_{dc,i}) = -\frac{2\,g_{dc}f_{dc}(e_{dc}N_0+I_{dc})}{(e_{dc}N_0+f_{dc}P_{dc,i}+I_{dc})^3} \le 0$.

Upon substituting $w(P_{dc,i})$ into Eq. (7), we find that the second derivative of $\tilde{r}_{d,i}$ is negative and hence $\tilde{r}_{d,i}$ is a concave function of $P_{dc,i}$. Following the composition rule of [32], which states that the sum of monotonically increasing and concave functions is also a concave function, we can now deduce that the OF of Eq. (5a) is concave in $P_{dc,i}$. Note that since $\tilde{r}_{d,i}$ relies on another variable $y_{dc,i}$, which is binary, we temporarily consider $y_{dc,i}$ to be a continuous variable lying within the interval [0, 1] and replace $P_{dc,i}$ by a new variable $z_{dc,i} = y_{dc,i}P_{dc,i}$. Using this temporary relaxation on $y_{dc,i}$, the constraints in Eq. (5) are seen to be convex in $\{y_{dc,i}, z_{dc,i}\}$, while $\tilde{r}_{d,i}(z_{dc,i})$ is concave, since $\tilde{r}_{d,i}(y_{dc,i}, z_{dc,i})$ is the perspective function of $\tilde{r}_{d,i}(z_{dc,i})$ [32]. Therefore, Eq. (5) preserves the convexity of the problem, since $\tilde{r}_{d,i}$ is concave with respect to both $y_{dc,i}$ and $z_{dc,i}$. □

Based on this analysis, we invoke the classic Lagrangian constrained optimization method and analytically characterise both the transmit power $\mathbf{P_{dc}}$ as well as the D2D-MU matching $\mathbf{y_{dc}}$ in following proposition.

Proposition 2: Assuming that the d^{th} D2D link reuses the RB of the c^{th} MU, the power allocation $P^*_{dc,i}$ for the D2D link is formulated as Eq. (8), as shown at the top of the next page, where $[a]^+$ denotes $\max\{0, a\}$ and $\boldsymbol{\lambda}, \boldsymbol{\mu}, \boldsymbol{\omega}, \boldsymbol{\gamma}$ are Lagrangian multipliers associated with Eq. (5d)-Eq. (5g) respectively. The D2D-MU matching $y^*_{dc,i}$ for a given power allocation of

$$P^*_{dc,i} = \left[\sqrt{\left(\frac{s^{(1)}_{dc}}{2\,s^{(0)}_{dc}}\right)^2 - \frac{s^{(2)}_{dc}(\lambda_{dc,i},\,\mu_{dc,i},\,\omega_i,\,\gamma_i)}{s^0_{dc}}} - \left(\frac{s^{(1)}_{dc}}{2\,s^{(0)}_{dc}}\right)\right]^+,$$

$$s^{(0)}_{dc} = (f_{dc} + g_{dc})f_{dc};$$

$$s^{(1)}_{dc} = (2\,f_{dc} + g_{dc})(I_{dc} + e_{dc}N_0);$$

$$s^{(2)}_{dc}(\lambda_{d,i},\,\mu_{d,i},\,\omega_i,\,\gamma_i) = (I_{dc} + e_{dc}N_0)^2 - \frac{g_{dc}(I_{dc} + e_{dc}N_0)g_c}{\ln(2)\left[\lambda_{d,i} + \mu_{d,i}\tau_i + \gamma_i x_c \frac{\alpha_c}{g_c} g^I_{dc} + \omega_i(1 - x_c)\sum_{p=1}^{P} \frac{x_p\alpha_p}{g_{pc}} g^I_{dc}\right]}. \tag{8}$$

$$H_{dc,i} = \eta_{dc,i} + (1 - \beta_c)\psi_{dc,i}$$

$$= \log_2\left(1 + \frac{g_{dc}P_{dc,i}}{e_{dc}N_0 + f_{dc}P_{dc,i} + I_{dc}}\right) - \left(\lambda_{d,i} + \mu_{d,i}\tau_i + \gamma_i x_c \frac{\alpha_c}{g_c} g^I_{dc} + \omega_i(1 - x_c)\sum_{p=1}^{P} \frac{\alpha_p x_p}{g_{pc}} g^I_{dc}\right) P_{dc,i}. \tag{10}$$

$P_{dc,i}$ is given by:

$$y^*_{dc,i} = 1, \quad d = \underset{\substack{1\le\hat{d}\le D\\ 1\le c\le C_{co}}}{\text{argmax}} \; H_{\hat{d}c,i};\; y^*_{dc,i} = 0,\; \forall \hat{d} \neq d, \tag{9}$$

where $H_{dc,i}$ is given in Eq. (10), as shown at the top of the this page.

Moreover, for orthogonal spectrum sharing ($\beta_c = 1$), C_{co} is an empty set and the constraint of Eq. (5c) is inactive, i.e. we have $\psi_{dc,i} = 0$. Hence, the above equation reduces to

$$y^*_{dc,i} = 1, \quad d = \underset{1\le\hat{d}\le D}{\text{argmax}} \; H_{\hat{d}c,i};\; y^*_{dc,i} = 0,\; \forall \hat{d} \neq d. \tag{11}$$

Proof: See Appendix B for proof. □

Remark 1: We can observe both from Eq. (9) as well as from Eq. (11) that the c^{th} MU's RB corresponding to the highest value of $H_{dc,i}$ will be reused by the d^{th} D2D link. According to Eq. (10), $H_{dc,i}$ depends on the different independent and identically distributed random channel gains. Therefore, practically speaking, the probability of having $H_{\hat{d}c,i} = H_{\tilde{d}c,i}$ where $\tilde{d} \neq d$ is infinitesimally low. Hence, the temporary relaxation imposed on $y_{dc,i}$ to be continuous variables lying in [0, 1] still produces a binary solution.

Based on the above analysis, we propose an iterative algorithm termed as the *joint optimization of the RB and of the power allocation (JORPA)*. This algorithm simultaneously derives the optimized transmit power of both the D2D links and that of the MUs along with D2D-MU matching relying on the idealistic setting of an off-line EH process, where the D2D links are perfectly aware of the energy arrival instants. This is formally stated in Algorithm 1. For a given power allocation of the D2D links obtained from Eq. (8) defined in line 31 of Algorithm 1, it allocates the adequate-quality cellular RBs to the D2D links according to Eq. (11) and/or Eq. (9), depending upon the specific spectrum sharing scenario considered, as given in lines 33-37. This algorithm minimises the dual problem of Eq. (5) by finding the optimal values of $\boldsymbol{\lambda_{d,i}}$, $\boldsymbol{\mu_{d,i}}$, $\boldsymbol{\gamma_i}$ and $\boldsymbol{\omega_i}$ using the popular bisection based search method employed for updating these multipliers in each of the four nested loops.

The Lagrangian multipliers $\boldsymbol{\gamma_i}$ and $\boldsymbol{\omega_i}$ are updated according to the maximum tolerable interference inflicted by the D2D links upon the MUs associated with the MBS (lines 19-25) or PBSs (Lines 11-17), respectively, which are then fed into the sub-algorithm. This sub-algorithm is constituted by a pair of nested loops, each updating the Lagrangian multipliers $\boldsymbol{\lambda_{d,i}}$ and $\boldsymbol{\mu_{d,i}}$ according to both the power budget and to the energy causality constraints of Eq. (5d) and Eq. (5e) at the D2D links, in lines 38-43 and 45-50 of Algorithm 1 respectively. Finally, the power allocation of the MUs associated with the MBS or PBSs is obtained using Eq. (15) and Eq. (16), respectively. The termination condition of this algorithm ensures that the assignment of the RBs to the D2D links and the power allocated both to the D2D links and to the MUs become sufficiently accurate by initializing the accuracy threshold ϵ to a small value at line 3 of Algorithm 1.

Now, according to Eq. (8) and Eq. (10), $P^*_{dc,i}$ and $H^*_{dc,i}$ are functions of the Lagrangian multipliers as well as the proposed JORPA algorithm requires upper bounds for Lagrangian multipliers (lines 6, 8, 27, 29) for initiating the optimization for our resource allocation problem. Hence, for the sake of achieving a faster convergence, we define the bounds of these multipliers in lemma 2.

Lemma 2: The optimal Lagrangian Multipliers $\boldsymbol{\lambda^*_{d,i}}$, $\boldsymbol{\mu^*_{d,i}}$, $\boldsymbol{\gamma^*_i}$ *and* $\boldsymbol{\omega^*_i}$ *lie in the interval* $[0, \lambda^{max}_{d,i}]$,$[0, \mu^{max}_{d,i}]$,$[0, \gamma^{max}_i]$ *and* $[0, \omega^{max}_i]$, *respectively, where upper bounds are given by,*

$$\lambda^{max}_{d,i} = \underset{1\le c\le C}{argmax}\left(\frac{g_{dc}}{\ln(2)(I_{dc} + e_{dc}N_0)}\right), \tag{12a}$$

$$\mu^{max}_{d,i} = \underset{1\le c\le C}{argmax}\left(\frac{g_{dc}}{\ln(2)\tau_i\,(I_{dc} + e_{dc}N_0)}\right), \tag{12b}$$

$$\gamma^{max}_i = \underset{\substack{1\le c\le C\\ 1\le d\le D}}{argmax}\left(\frac{g_{dc}g_c}{\ln(2)(I_{dc} + e_{dc}N_0)x_c\alpha_c g^I_{dc}}\right), \tag{12c}$$

Algorithm 1 Algorithm for Joint Optimization of RB and Power Allocation (JORPA)

Input: P_C^{max}, P_P^{max}, P_D^{max} $\forall d$, R_c, g_c, g_c^I, x_c, β_c $\forall c$; x_{pc} $\forall$ MUs associated with PBS; g_{dc}, g_{dc}^I, g_{cd}^I, g_{pc}, g_{pc}^I, g_{pd}^I $\forall c, d, p$; $E_{d,i}$ $\forall d, i, t_i$ $\forall i$ T_{max}, K, N_0, C_{co}.

Output: $P_{dc,i}^*$, $y_{dc,i}^*$ $\forall c, d, i$, P_c^*, P_p^* $\forall c$ $\forall p$.

Initialize: Set accuracy ϵ, $i = 1$, $P_c^I = \frac{P_C^{max}}{\sum_{c=1}^{C} x_c}$ and $P_p^I = \frac{P_p^{max}}{\sum_{c=1}^{C} x_{pc}}$ for calculating I_M and I_P.

Let $P_{sur} = P_C^{max} - \sum_{c=1}^{C} x_c \frac{\alpha_c}{g_c} \left[\sum_{p=1}^{P}((1-\beta_c x_c)I_P) + N_0\right]$ and $P_{sur,P} = P_P^{max} - \sum_{c=1}^{C}(1 - x_c)\frac{x_{pc}\alpha_p}{g_{pc}}[(\beta_c x_c + (1-\beta_c))I_M + N_0]$.

for $(i = 1 : K)$ **do**

  Set $\gamma_a = 0$, $\gamma_b = \gamma_i^{max}$; $n = 1$, $\gamma_i(n) = \frac{(\gamma_a+\gamma_b)}{2}$.

  while $|\gamma_a - \gamma_b| > \epsilon$ **do**

    Set $\omega_a = 0$, $\omega_b = \omega_i^{max}$; $o = 1$, $\omega_i(o) = \frac{(\omega_a+\omega_b)}{2}$.

    while $|\omega_a - \omega_b| > \epsilon$ **do**

      Find $\mu_{d,i}^*$, $\lambda_{d,i}^*$, $P_{dc,i}^*$, $y_{dc,i}^*$ $\forall d, c$ for a given $\gamma_i(n)$ and $\omega_i(o)$ using Sub-Algorithm below.

      Let $P'_{sur,P} = \sum_{d=1}^{D}\sum_{c=1}^{C}(1 - x_c)\frac{x_p\alpha_p}{g_{pc}} y_{dc,i} P_{dc,i} g_{dc}^I$

      if $P'_{sur,P} \leq P_{sur,P}$ **then**

        $\omega_b = \omega_i(o)$;

      else

        $\omega_a = \omega_i(o)$;

      end if

      Update $o = o + 1$, $\omega_i(o) = \frac{(\omega_a+\omega_b)}{2}$.

    end while

    Let $P'_{sur} = \sum_{d=1}^{D}\sum_{c=1}^{C} x_c \frac{\alpha_c}{g_c} y_{dc,i} P_{dc,i} g_{dc}^I$

    if $P'_{sur} \leq P_{sur}$ **then**

      $\gamma_b = \gamma_i(n)$;

    else

      $\gamma_a = \gamma_i(n)$;

    end if

    Update $n = n + 1$, $\gamma_i(n) = \frac{(\gamma_a+\gamma_b)}{2}$.

  end while

Sub Algorithm:

  Initialize: $m = 1$, $\mu_a = 0$, $\mu_b = \mu_{d,i}^{max}$, $\mu_{d,i}(m) = \frac{(\mu_a+\mu_b)}{2}$.

  while $|\mu_a - \mu_b| > \epsilon$ **do**

    Initialize: $l = 1$, $\lambda_a = 0$, $\lambda_b = \lambda_{d,i}^{max}$, $\lambda_{d,i}(l) = \frac{(\lambda_a+\lambda_b)}{2}$, $\tau_i = t_i - t_{i-1}$ $\forall i$.

    repeat

      Calculate $P_{dc,i}^*$ $\forall d, c, i$ with the given $\gamma_i(n)$, $\omega_i(o)$, $\mu_{d,i}(m)$ and $\lambda_{d,i}(l)$ via Eq. (8).

      Compute $H_{dc,i}$ for any d, c via Eq. (10).

      if $\beta_c = 0$ **then**

        Match d^{th} D2D link with c^{th} MU using to Eq. (9)

      else

        Match d^{th} D2D link with c^{th} MU using to Eq. (11)

      end if

      if $(\sum_{c=1}^{C} y_{dc,i} P_{dc,i} \leq P_D^{max})$ **then**

        $\lambda_b = \lambda_{d,i}(l)$;

      else

        $\lambda_a = \lambda_{d,i}(l)$;

      end if

      Update $l = l + 1$, $\lambda_{d,i}(l) = \frac{(\lambda_a+\lambda_b)}{2}$.

    until $|\lambda_a - \lambda_b| < \epsilon$ $\forall d, i$

    if $\sum_{\kappa=1}^{i}\sum_{c=1}^{C} y_{dc,\kappa} P_{dc,\kappa} \tau_\kappa > \sum_{\kappa=0}^{i-1} E_{d,\kappa}$ **then**

      $\mu_b = \mu_{d,i}(m)$;

    else

      $\mu_a = \mu_{d,i}(m)$;

    end if

    Update $m = m + 1$, $\mu_{d,i}(m) = \frac{(\mu_a+\mu_b)}{2}$.

  end while

end for

Finally obtain P_c^* $\forall$ $y_{dc,i} = 1$ and $x_c = 1$ using Eq. (15) and P_p^* $\forall$ $y_{dc,i} = 1$ and $x_c = 0$ using Eq. (16).

$$\omega_i^{max} = \underset{\substack{1\leq c\leq C \\ 1\leq d\leq D}}{argmax} \left(\frac{g_{dc}}{\ln(2)(I_{dc}+e_{dc}N_0)(1-x_c)\sum_{p=1}^{P}\frac{xp\alpha_p}{g_{pc}} g_{dc}^I} \right). \tag{12d}$$

Proof: See Appendix C for proof. □

The mathematical proof of convergence of our Algorithm 1 has been omitted from this treatise because our algorithm invokes the bisection search method for obtaining the optimal values of Lagrangian multipliers, whose convergence is shown in [33], [34]. However, in Fig. 4, we present the convergence of our algorithm for each energy harvesting epoch under all the spectrum sharing strategies considered in this treatise. This algorithmic convergence is achieved for each Monte-Carlo run before obtaining the final results by averaging over the number of Monte-Carlo runs of simulation. It can be observed that as the number of iterations in the algorithm increases, the sum-rate of the D2D links becomes constant for all the three spectrum sharing schemes.

IV. HEURISTIC SOLUTIONS

Since the complexity[7] of the optimized solution is potentially excessive owing to the presence of four nested loops in the proposed JORPA Algorithm 1, we conceived the following heuristic methods, where the optimization variables of $\mathbf{P_{dc}}$ and $\mathbf{y_{dc}}$ are reduced to a single one, while heuristically obtaining the other variables. The details of the methods are as follows:

- *Equal Power Allocation (EPA)*: In this method, we invoke a simple plausible *harvesting and dissipation*

[7]The complexity analysis of the JORPA and heuristic algorithms is beyond the scope of this paper.

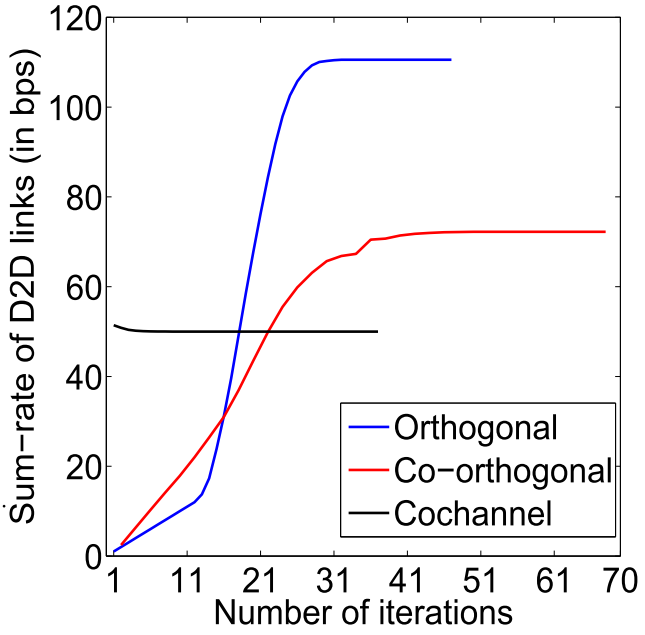

FIGURE 4. Convergence of our algorithm as a sum-rate of D2D links with respect to the number of iterations. Here $P = 1$, $D = 8$, $C = 10$, $B = 20$dB, $R_p = 4$bps/Hz, and $R_c = 8$bps/Hz.

strategy for allocating power to the D2D link. In this harvesting and dissipation strategy, the transmit power of the D2D links is obtained by equally distributing the energy harvested to the reused RBs without violating the maximum power budget of D2D transmission, which results in satisfying the constraints given in Eq. (5d) and Eq. (5e) heuristically. Based on this heuristic power allocation, the D2D-MU matching is then optimized using the reduced complexity optimization problem by satisfying the constraints Eq. (5b) and Eq. (5c). Moreover, the maximum tolerable interference level of each of the BSs is never exceeded, which is ensured by disabling the D2D transmissions on the RBs of specific BSs, when the constraints of Eq. (5f)-Eq. (5g) would become violated.

- *Random D2D-MU Matching (RM)*: According to this method, we optimize the power allocation by the random mapping of the D2D links to the MU's resource blocks, while ensuring that the constraints of Eq. (5b) and Eq. (5c) are still satisfied. The transmit power is then optimized under the constraints of Eq. (5d) and Eq. (5e), where again, the maximum tolerable interference constraints of the BSs are never exceeded, which is guaranteed by setting the D2D-MU matching to zero for the specific DL RBs of the BSs when they are about to be violated.
- *Maximum Distance D2D-MU Matching (MDM)*: According to this method, we match the D2D links to that specific MU's RB, which is at the largest distance from the D2D link in order to reduce the interference it inflicts upon the MUs, while satisfying the constraints of Eq. (5b) and Eq. (5c). The transmit power is then optimized under the constraints of Eq. (5d) and Eq. (5e), where again, the maximum tolerable interference constraints of the BSs are never exceeded, which is guaranteed by setting the D2D-MU matching to zero for the specific DL RBs of the BSs, when the constraints would become violated.

TABLE 1. Parametric Settings for our simulations.

Parameter	Value
Maximum amount of energy Harvested, E_{max}	100 mJ
Rate of energy harvesting, λ	3 mJ/second
Radius of cell, R	500m
Power Budget for MBS, P_C^{max}	46dBm
Power Budget for PBS, P_P^{max}	30dBm
Power Budget for D2D links, P_d^{max}	20dBm
Target throughput for MUs associated with MBS R_c	8bps/Hz
Target throughput for MUs when associated with PBS R_p	4bps/Hz
Interference-threshold for D2D links I_{Th}	40dBm
Biasing Factor for PBS B	20dB
Path-loss exponent for D2D TX -D2D RX/MU, α_d	4
Path-loss exponent for PBS - MU/D2D RX, α_p	3.5
Path-loss exponent for MBS - MU/D2D RX, α_c	3
Thermal noise density, N_0	−174dBm/Hz
Bandwidth of System	10MHz

V. SIMULATION RESULTS

In this section, we analyse the performance of both our optimal algorithm as well as of our heuristic methods for the achievable D2D sum-rate with the deadline of $T = 10$ seconds, where the D2D links have an energy harvesting capability and reuse the radio resources of the MUs associated with the MBS or PBSs in different spectrum sharing scenarios. The EH processes of each D2D link are independent and they are composed of two random processes: the energy arrival obeys a uniform distribution between $[0, E_{max}]$ mJoule and the arrival instants are defined as Poisson-distributed at a rate of λ mJoule/s. The MBS is located at the origin, while the PBSs are distributed randomly in the cell of radius R, where the BSs are assumed to utilise all the radio resources allocated to them all the time. The parametric settings for the quantitative analysis of this treatise are given in Table 1. Based on the difference in the power budgets of the BSs given in Table 1, the throughput requirements are different for the MUs associated with the MBS and for those associated with the PBSs. The system is comprised of uniformly distributed MUs and D2D links, where the bias B for the MU association as well as interference-threshold I_{Th} for D2D links, are also set to those in Table 1, unless otherwise mentioned. The channels obey i.i.d. Rayleigh distribution and a path-loss model having different path-loss exponents due to the different propagation environments encountered in the different scenarios, which are set according to Table 1 [29], [35], [36]. The distance d_l between the D2D pair is set to vary in the interval of $[20, 40]$m. Our simulation results quantify the D2D sum-rate for different parameter settings, such as those of the D2D interference-threshold as well as bias for received signal strength from PBS, of the throughput threshold of the MUs associated with either the MBS or PBSs, of the number

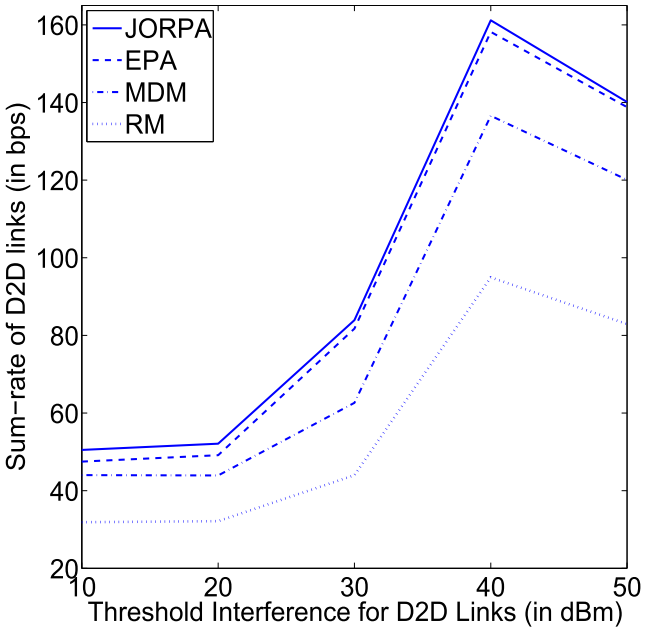

FIGURE 5. Effect of the interference-threshold for D2D links from the PBS on the D2D sum-rate. Here $P = 1$, $D = 8$, $C = 10$, $B = 20$dB, $R_P = 4$bps/Hz, and $R_C = 8$bps/Hz.

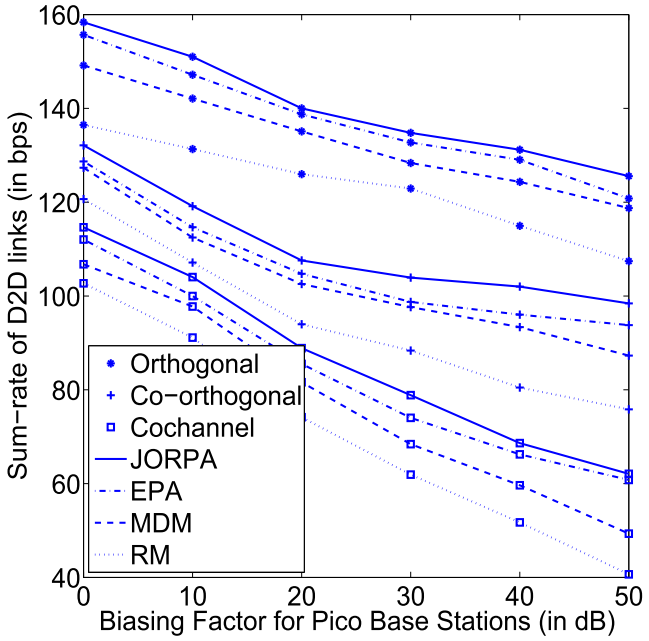

FIGURE 6. Impact of varying the number of D2D links on the D2D sum-rate. Here $P = 1$, $C = 10$, $D = 8$, $I_{Th} = 40$dBm, $R_C = 8$bps/Hz and $R_P = 4$bps/Hz.

of MUs as well as of the number of PBSs for different channel deployment schemes at the BSs.

Our first aim is to find the optimal threshold of the D2D links w.r.t. the interferers for the sum-rate maximization of the D2D links in the proposed co-orthogonal spectrum sharing scenario, where the interference-threshold, I_{Th}, is used for defining the interference-dependent switching of D2D links from the ideal scenario of only reusing RBs orthogonally to the aggressive co-channel reuse. Therefore, in Fig. 5, we analyse the D2D sum-rate for different values of the threshold I_{Th}. It can be observed from Fig. 5 that as the interference-threshold of the D2D links increases, the D2D sum-rate increases. This is because the system evolves from operating in completely co-channel fashion towards gradual orthogonal deployment, where the interference experienced by the D2D links in the former scenario is higher than in the latter one owing to the interfering DL transmission from all the active BSs at a time instant. Hence, for co-channel deployment the sum-rate of the D2D links is achieved, when we have $I_{Th} = 0$ dBm, while in the orthogonal scenario it is achieved, when we have $I_{Th} \geq (P_C^{max} + P_P^{max})$ dBm. Moreover, when $I_{Th} \in (0, P_C^{max} + P_P^{max})$ dBm, upon increasing the threshold, the number of D2D links reusing the RBs of the orthogonal sub-band is increased. Hence reduced interference is imposed, thereby increasing the sum-rate of D2D links. However, increasing the threshold further, $I_{Th} > 40$dBm results in a sum-rate reduction for the D2D links, which might be due to the fact that the number of D2D links reusing the orthogonal sub-bands has been increased, but the number of MUs using RBs within this sub-band still remained the same. This in turn means that there is a reduction in the number of orthogonal RBs available for reuse upon increasing the number of D2D links relying on orthogonal reuse. This results in a sum-rate reduction for the D2D links. We also analysed our heuristic methods upon varying the interference-threshold. We observe in Fig. 5 that the EPA performs similarly to our proposed JORPA algorithm of Algorithm 1, achieving approximately 96% of the sum-rate achieved by JORPA at a substantially lower complexity. On the other hand, the RM algorithm performs worse than the MDM algorithm, since in MDM, the D2D-MU matching is based on the maximum distance, which tends to reduce the interference imposed on the MUs, thereby supporting a higher D2D transmission power. Hence a better sum-rate is observed in Fig. 5 for the latter scheme. Furthermore, both the MDM and RM algorithm perform worse than the JORPA algorithm as well as than the EPA algorithm, which demonstrates the importance of the optimization discussed in this treatise. It also indicates that the specific choice of the D2D-MU matching is more crucial for this sum-rate maximization. Based on the performance results of Fig. 5, it is reasonable to set $I_{Th} = 40$ dBm for co-orthogonal deployment, since this choice supports a higher sum-rate for the D2D links than other values of the threshold.

We then analyse the impact of varying the biasing factor B of the PBSs on the D2D sum-rate in Fig. 6. It can be clearly observed that upon increasing the biasing factor, the D2D sum-rate is reduced for all the three spectrum sharing strategies. The reason behind this trend is that upon increasing the biasing factor, the number of MUs associated with PBSs is increased, which in turn implies that the interference imposed by the PBSs is reduced. By conrast, the interference inflicted by the MBS (which has a higher power budget) is increased

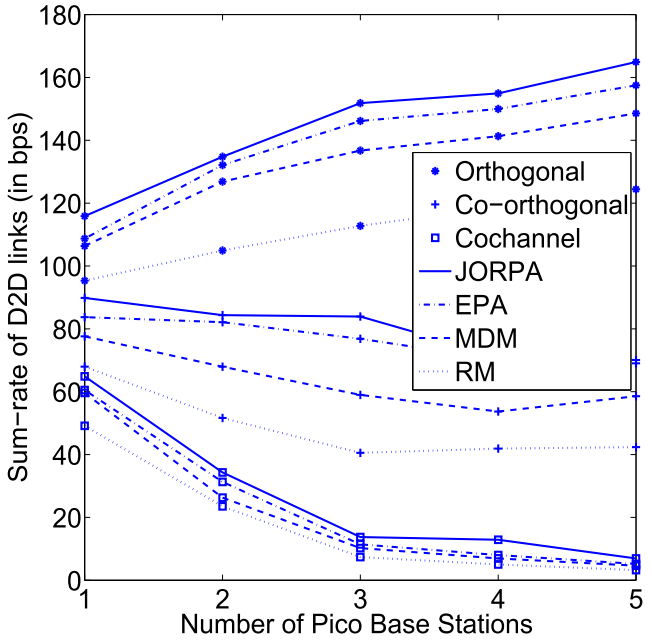

FIGURE 7. Impact of varying the number of Pico Base stations on the D2D sum-rate. Here $D = 8$, $C = 10$, $I_{Th} = 40$dBm, $B = 20$dB, $R_p = 4$bps/Hz and $R_c = 8$bps/Hz.

owing to the equal distribution of power, thereby increasing the overall interference experienced by the D2D links, which in turn results in their lower sum-rate. However, the orthogonal sharing performs best owing to the reduced interference inflicted upon the D2D links, when compared to the other two strategies. Moreover, upon comparing the co-channel and co-orthogonal spectrum sharing, it can be seen from Fig. 6 that the co-orthogonal regime performs better than the co-channel solution. This trend is due to the availability of RBs suffering from lower interference for reuse by the D2D links due to the resource partitioning into two sub-bands for supporting both orthogonal and co-channel RBs for DL transmission to the MUs in the former case. Again, our heuristic methods were analysed and it was observed that the EPA achieves 96% of the optimal sum-rate, while the other two heuristic algorithms perform worse than the JORPA algorithm and the EPA, which in turn shows that it is necessary to carefully optimize the D2D-MU matching for the sake of sum-rate maximization, as detailed in this treatise. Based on the performance results of Fig. 6, it is reasonable to set $B = 20$ dB, since this supports a better load balancing between the MBS and the PBSs than $B = 0$ or 10 dB, while simultaneously supporting a higher sum-rate for the D2D links than higher values of the biasing factor.

Fig. 7 represents the D2D sum-rate versus the number of PBSs. As the number of PBSs increases, there is a reduction in the traffic on the MBS, which implies that the MUs association with the PBSs increases, hence the transmission power of the PBSs decreases, which in turn reduces the amount of interference experienced by the D2D links from the PBSs. However, the transmit power of the MBS increases owing to the equal power distribution, as discussed in Section III. Therefore, the orthogonal channel deployment performs best, since the D2D links suffer from the interference arriving either from the MBS or PBSs and given the increased number of the PBSs, more MUs are associated with PBSs. Hence, when the D2D links reuse the RBs of MUs associated with PBSs, the interference is further reduced, thereby increasing their sum-rate. However, in case of co-channel deployment the sum-rate decreases, since even though in the presence of more PBSs the MUs tend to become associated with PBSs, which results in a reduction of their transmit power, but at the same time the MBS also shares the spectral resources with PBSs, which results in an increased MBS transmit power owing to its reduced traffic load. Hence, the overall interference experienced by the D2D links is increased due to the co-channel sharing, thereby reducing their sum-rate in the presence of more PBSs. It can also be seen from Fig. 7 that the co-orthogonal deployment follows similar trends of co-channel deployment owing to the increased interference suffered by the D2D links reusing the RBs in the co-channel sub-band. Nonetheless, it has a better performance than co-channel deployment which is an explicit benefit of partitioning the resources into orthogonal and co-channel sub-bands as well as a benefit of the improved chances of the D2D links becoming matched with MUs supported in orthogonal sub-bands, which reduces the interference. Here again, as expected, our heuristic methods exhibit similar trends, emphasizing the need for optimization, especially that of the D2D-MU matching parameter. Note that for simplicity, we will only present results for the EPA and MDM heuristic algorithms that perform better than the RM heuristic algorithm.

The D2D sum-rate recorded is reduced in Fig. 8 for different values of the throughput requirements of the MUs associated with the MBS, when the throughput threshold of the MUs served by PBSs is fixed. As expected, a diminishing trend is observed upon increasing the throughput threshold of the MUs associated with the MBS, because the power of the MBS transmitted to the MUs should be higher for the sake of increasing the throughput, while a reduced interference should be inflicted upon the MUs, which in turn implies that the interference imposed on the D2D links by the MBS increases, while its transmit power has to be reduced in order to meet the throughput requirements. Moreover, the orthogonal deployment performs better than the other two deployments, since the D2D links are interfered only by a single BS at any particular instant, depending on their D2D-MU matching invoked for resource reuse. On the other hand, the co-orthogonal regime performs better than the co-channel deployment, because in the former case the MUs associated with the MBS can either be deployed in an orthogonal or in a co-channel sub-band reuse pattern. Hence, in order to maximize the D2D sum-rate for meeting a higher throughput constraint, depending on their threshold I_{Th}, some D2D links tend to reuse the resources of the MUs supported by orthogonal sub-band, which in turn improves the over-all sum-rate in the

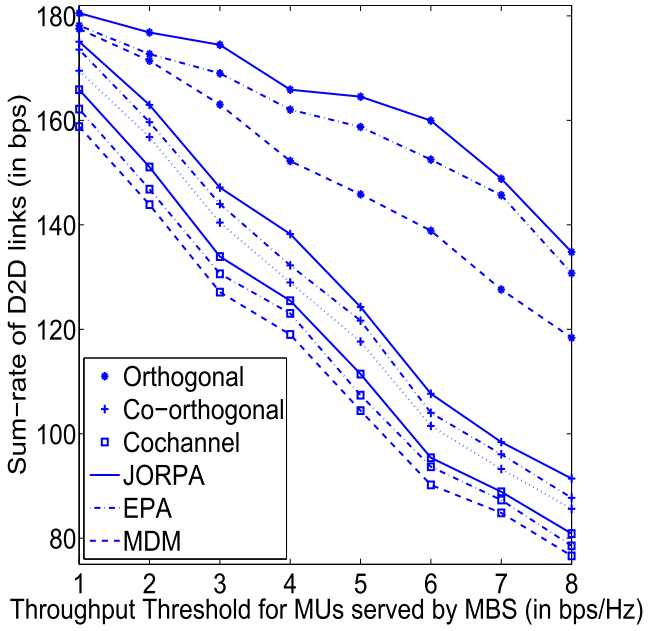

FIGURE 8. Impact of the Quality of Service threshold of MU associated with MBS on the D2D sum-rate. Here $P = 1$, $D = 8$, $C = 10$ $I_{Th} = 40$dBm, $R_p = 4$bps/Hz and $B = 20$dB.

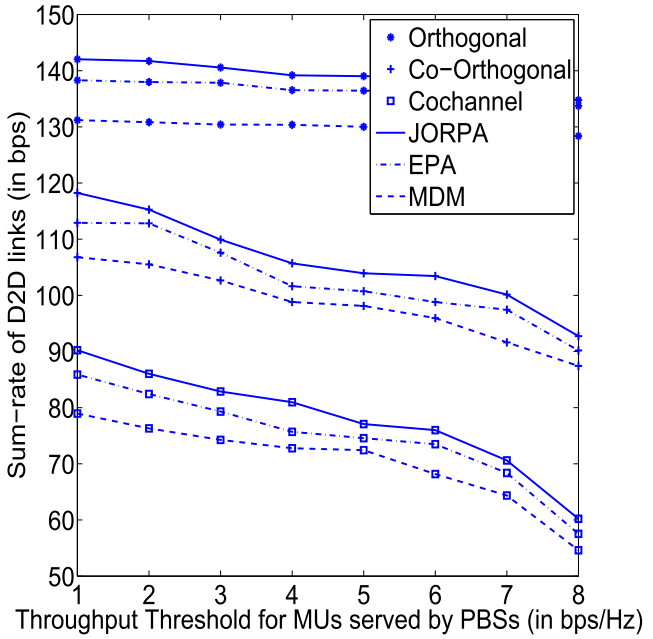

FIGURE 9. Impact of the Quality of Service threshold of the MU associated with PBSs on the D2D sum-rate. Here $P = 1$, $D = 8$, $C = 10$ $I_{Th} = 40$dBm, $R_c = 8$bps/Hz and $B = 20$dB.

former case. Again, similar to our previous results seen in Fig. 5 - Fig. 7, our heuristic methods follow their expected trend Fig. 8

The achievable D2D sum-rate is analysed in Fig. 9 for different values of the throughput target of the MUs associated with the PBS, when that of the MUs associated with the MBS is fixed. Interestingly, it can be observed that upon increasing the throughput requirement of the MUs associated with the PBSs, we observe that the D2D sum-rate is reduced, albeit at a slower rate. The reason behind this trend is the lower power budget of the PBSs in our system setting. This suggests that for increasing the throughput threshold of the MUs associated with the PBS, the transmit power of the PBS should increase, while the interference experienced at these MUs should be reduced. However, the transmit power of the PBS is limited by its power budget. Hence, the PBS does not increase the interference it imposes on the D2D links beyond a certain limit, which in turn results in a slower rate of decrease in the sum-rate of D2D links, despite increasing the throughput of the MUs associated with the PBS. Moreover, the orthogonal deployment performs better than the other two deployments owing to transmission only by a single BS on each RB, while the co-orthogonal assignment performs better than the co-channel deployment, since it subsumes both the orthogonal and co-channel regimes. Again, the pair of heuristic methods that follow similar trends in Fig. 9 to those of Fig. 5 - Fig. 8, further supporting the fact that using a beneficial D2D-MU matching is important for the maximization of the D2D sum-rate.

Finally, Fig. 10 characterizes the effect of varying the number of MUs on the D2D sum-rate. As expected, upon

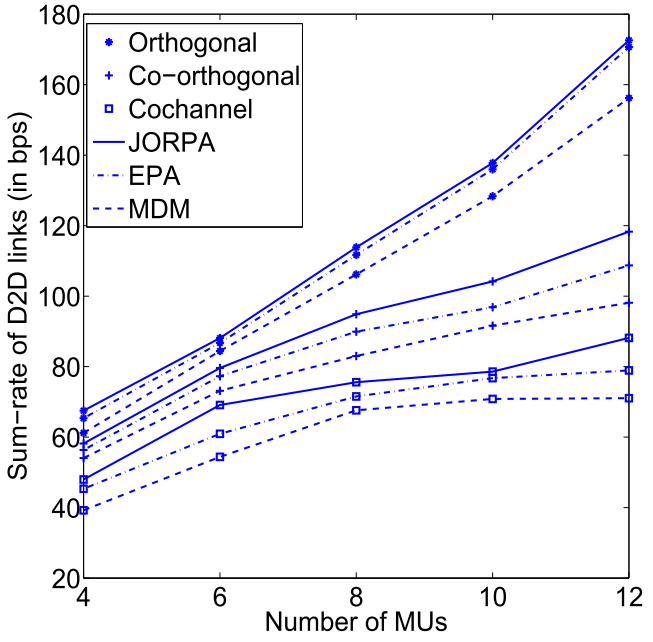

FIGURE 10. Impact of varying the number of MUs on the D2D sum-rate. Here $P = 1$, $D = 8$, $I_{Th} = 40$dBm, $B = 20$dB, $R_p = 4$bps/Hz and $R_c = 8$bps/Hz.

increasing the number of MUs, the sum-rate of D2D links is increased for all the three channel sharing scenarios. This trend is observed due to the fact that upon increasing the number of MUs, the number of RBs available for D2D reuse is also increased. Hence the D2D links receive more resources for transmitting their information, thereby enhancing their overall sum-rate. The orthogonal channel deployment

TABLE 2. Throughput achieved for MUs under different spectrum sharing schemes when JORPA is used for resource allocation on introduction of D2D links.

Spectrum Sharing	Achieved R_c bps/Hz	Achieved R_p bps/Hz
Co-channel	7.99	3.98
Co-orthogonal	12.16	4.97
orthogonal	8.97	4.16

performs best, followed by the co-orthogonal and co-channel deployment owing to the different levels of interference experienced by the D2D links under the different spectrum sharing strategies. Bearing in mind the results Fig. 5 - Fig. 9, our heuristic methods are also expected to follow similar trends in Fig. 10.

Table 2 shows the throughput achieved for the MUs associated with MBS or PBSs for the different schemes on the introduction of D2D communication, when JORPA is employed for resource allocation. The throughput threshold for MUs associated with MBS is set to $R_c = 8$ bps/Hz, while that with PBSs is set to $R_p = 4$ bpz/Hz. We can observe in Table 2 that for co-channel deployment, throughput achieved for MUs is approximately equivalent to the threshold, while that for the other two deployments surpasses the minimum required throughput threshold. The reason behind this trend is the presence of D2D communication that is reusing the DL resources of MUs imposing additional interference in the existing infrastructure. This implies that for co-channel scenario that already suffers from higher interference is further introduced with interference due to D2D transmission and thus is unable to achieve throughput threshold. Moreover, our proposed co-orthogonal scheme is capable of achieving 50% higher than the required throughput threshold for the MUs associated with the MBS, while only 24% higher than that for the MUs associated with the PBSs. This is due to the higher power budget of the MBS than that of the PBSs as well as due to the interference based switching adopted by the D2D links for reusing the DL resources in either the co-channel or the orthogonal sub-band. Table 2 reveals that the presence of D2D communication reduces the throughput experienced by the MUs for co-channel spectrum sharing, while our proposed scheme as well as the orthogonal deployment is still capable of achieving the throughput threshold.

VI. CONCLUSIONS

Heterogeneous downlink resource reuse solutions were investigated, a two-tier scenario, where the D2D links reuse the downlink cellular RBs. The D2D links are powered by scavenging energy from the surroundings. An optimization problem was constructed with the objective of maximizing the D2D sum-rate, without unduly degrading the throughput of the cellular communication. In order to solve the resultant non-convex problem, it was first transformed to the corresponding convex problem by defining the optimal downlink transmit power of each MU for satisfying the throughput constraints. We then invoked the classic Lagrangian constrained optimization method for analytically deriving the resource reuse and power allocation for both the D2D links as well as for the MUs, which was achieved by relaxing the D2D-MU matching variables for our non-causal EH process. An algorithm termed as *Joint optimization of RB and power allocation (JORPA) for D2D links* was then proposed, relying on the analytical results of the joint optimization of the three spectrum sharing schemes. In order to circumvent the potentially excessive complexity of our proposed algorithm, we also conceived three heuristic methods, where either the D2D power allocation or the D2D-MU matching was optimized, while other one of the two parameters was heuristically defined. Our simulation results reveal that the D2D sum-rate is the highest for the orthogonal spectrum sharing and the lowest for the co-channel arrangement, as determined by the amount of interference experienced by the D2D links. The presence of D2D communication effects the throughput experienced by MUs due to increased interference which is observed most in co-channel sharing followed by orthogonal sharing while our proposed co-orthogonal regime is capable of achieving substantially higher throughput for the MUs than the threshold. Furthermore, our proposed co-orthogonal spectrum sharing scheme strikes a balance between these two richly investigated spectrum sharing scenarios by adopting the best features of these two schemes. This is an explicit benefit of the reduction in interference by the orthogonal sharing, while improving the bandwidth exploitation with the aid of co-channel spectrum sharing. Finally, our analysis of the heuristic methods underlined the importance of optimization in the system. Specifically, optimization of the D2D-MU matching variable is crucial for the maximization of the D2D sum-rate, as revealed by our EPA Algorithm, which achieves 96% of the sum-rate attained by our JORPA algorithm at a fraction of its complexity.

APPENDIX A

Since, the transmit powers of the MBS and PBSs are optimized using the problem given in Eq. (4) are unknown, it is necessary to consider a reasonable value for the interferences I_M and I_P for the sake of transforming the problem into a more tractable form. Therefore, we consider an equal power distribution[8] at all the BSs. Hence we arrive at the interfering powers of the PBSs and MBS in the form of, $P_p^I = \frac{P_P^{max}}{\sum_{c=1}^{C} x_{pc}}$ and $P_c^I = \frac{P_C^{max}}{\sum_{c=1}^{C} x_c}$, respectively. Assuming that the RB of the MU c associated with the MBS is reused by the d^{th} D2D link, i.e. we have $x_c = 1$, $y_{dc,i} = 1$, from Eq. (2), we arrive at

$$P_c \geq \frac{\alpha_c}{g_c}\left(N_0 + g_{dc}^I P_{dc,i} + (1 - \beta_c x_c) I_P\right), \tag{13}$$

where $\alpha_c = 2^{R_c} - 1$. Similarly, assuming $x_c = 0$, $x_{pc} = 1$, $y_{dc,i} = 1$, which means that the d^{th} D2D link reuses the c^{th} MU's RB that is served by the p^{th} PBS, from Eq. (3), we arrive

[8]Dynamic power allocation is a reasonable method to allocate power in downlink at BSs, however, in this work, we consider equal power allocation for the sake of not over complicating the problem at hand.

$$p^*_{dc,i} \geq 0$$

$$\left[\sqrt{\left(\frac{s^{(1)}_{dc}}{2\,s^{(0)}_{dc}}\right)^2 - \frac{s^{(2)}_{dc}(\lambda_{dc,i},\,\mu_{dc,i},\,\gamma_{dc,i})}{s^{0}_{dc}}} - \left(\frac{s^{(1)}_{dc}}{2\,s^{(0)}_{dc}}\right)\right]^{+} \geq 0$$

$$(I_{dc}+e_{dc}N_0)^2 - \frac{g_{dc}(I_{dc}+e_{dc}N_0)g_c}{\ln(2)\left[\lambda_{dc,i}+\mu_{dc,i}\tau_i+\gamma_i x_c\frac{\alpha_c}{g_c}g^I_{dc}+\omega_i(1-x_c)\sum_{p=1}^{P}\frac{x_p\alpha_p}{g_{pc}}g^I_{dc}\right]} \leq 0.$$

at

$$P_p \geq \frac{\alpha_p}{g_{pc}}\left(N_0 + g^I_{dc}P_{dc,i} + [\beta_c x_c + (1-\beta_c)]I_M\right), \quad (14)$$

where $\alpha_p = 2^{R_p} - 1$. Since increasing P_c and P_p monotonically decreases the OF value of Eq. (4a) for a fixed $P_{dc,i}$, the optimal value of P_c and P_p maximising the D2D sum-rate must be attained by satisfying the equality in Eq. (13) and Eq. (14), i.e. we have,

$$P^*_c = \frac{\alpha_c}{g_c}\left(N_0 + g^I_{dc}P_{dc,i} + (1-\beta_c x_c)I_P\right) \quad (15)$$

and,

$$P^*_p = \frac{\alpha_p}{g_{pc}}\left(N_0 + g^I_{dc}P_{dc,i} + [\beta_c x_c + (1-\beta_c)]I_M\right). \quad (16)$$

Thus, the explicit throughput constraints are eliminated using the above modifications and substituting P^*_c and P^*_p into the OF of Eq. (4a) yields the transformed OF given in Eq. (6). Similarly, we can substitute P^*_c and P^*_p into the constraint of Eq. (4g) and Eq. (4f) to arrive at the modified constraint of Eq. (5g) and Eq. (5f). Thus the transformed and more tractable form of the original problem Eq. (4) can be written as Eq. (5).

APPENDIX B

In order to derive the results of this lemma, the KKT conditions of Eq. (5) were examined. The Lagrangian function for the optimization of the equivalent problem of Eq. (5) is defined as follows:

$$\begin{aligned}
\mathcal{L} = &-\sum_{i=1}^{K}\sum_{d=1}^{D}\sum_{c=1}^{C} y_{dc,i} \\
&\times\log_2\left(1+\frac{g_{dc}P_{dc,i}}{e_{dc}N_0+f_{dc}P_{dc,i}+I_{dc}}\right) \\
&+\sum_{i=1}^{K}\sum_{c=1}^{C}\eta_{dc,i}\left(\sum_{d=1}^{D}y_{dc,i}-1\right) \\
&+\sum_{i=1}^{K}\psi_{dc,i}\left(\sum_{c=1\in C_{co}}\sum_{d=1}^{D}(1-\beta_c)y_{dc,i}-1\right) \\
&+\sum_{i=1}^{K}\sum_{d=1}^{D}\lambda_{d,i}\left(\sum_{c=1}^{C}y_{dc,i}P_{dc,i}-P^{max}_D\right) \\
&+\sum_{i=1}^{K}\sum_{d=1}^{D}\mu_{d,i} \\
&\times\left(\sum_{\kappa=1}^{i}\sum_{c=1}^{C}y_{dc,\kappa}P_{dc,\kappa}\tau_\kappa-\sum_{\kappa=0}^{i-1}E_{d,\kappa}\right) \\
&+\sum_{i=1}^{K}\sum_{p=1}^{P}\omega_i \\
&\times\left(\sum_{d=1}^{D}\sum_{c=1}^{C}(1-x_c)x_{pc}\frac{\alpha_p}{g_{pc}}y_{dc,i}P_{dc,i}g^I_{dc}\right. \\
&-\left(P^{max}_p-\sum_{c=1}^{C}(1-x_c)x_{pc}\frac{\alpha_p}{g_{pc}}\right. \\
&\left.[(\beta_c x_c+(1-\beta_c))I_M+N_0])\right) \\
&+\sum_{i=1}^{K}\gamma_i\left(\sum_{d=1}^{D}\sum_{c=1}^{C}x_c\frac{\alpha_c}{g_c}y_{dc,i}P_{dc,i}g^I_{dc}\right. \\
&\left.\left.-\left(P^{max}_C-\sum_{c=1}^{C}x_c\frac{\alpha_c}{g_c}[(1-\beta_c x_c)I_P)+N_0]\right)\right),
\end{aligned} \quad (17)$$

where $\eta_{dc,i}$, $\psi_{dc,i}\lambda_{d,i}$, $\mu_{d,i}$, γ_i and ω_i are Lagrangian multipliers associated with the constraints of Eq. (5b), Eq. (5c), Eq. (5d), Eq. (5e), Eq. (5g) and Eq. (5f), respectively. Now, evaluating the differentiation of Lagrangian function with respect to $y_{dc,i}$ and equating them to zero, we get:

$$\begin{aligned}
&\frac{\partial\mathcal{L}}{\partial y_{dc,i}} = 0 \\
&-\log_2\left(1+\frac{g_{dc}P_{dc,i}}{e_{dc}N_0+f_{dc}P_{dc,i}+I_{dc}}\right)+\eta_{dc,i}+(1-\beta_c)\psi_{dc,i} \\
&+\left(\lambda_{d,i}+\mu_{d,i}\tau_i+\omega_i\,(1-x_c)x_{pc}\frac{\alpha_p}{g_{pc}}g^I_{dc}+\gamma_i x_c\frac{\alpha_c}{g_c}g^I_{dc}\right) \\
&\times P_{dc,i} = 0 \\
&\eta_{dc,i}+(1-\beta_c)\psi_{dc,i} = \log_2\left(1+\frac{g_{dc}P_{dc,i}}{e_{dc}N_0+f_{dc}P_{dc,i}+I_{dc}}\right) \\
&-\left(\lambda_{d,i}+\mu_{d,i}\tau_i+\omega_i\,(1-x_c)x_{pc}\frac{\alpha_p}{g_{pc}}g^I_{dc}+\gamma_i x_c\frac{\alpha_c}{g_c}g^I_{dc}\right)P_{dc,i}.
\end{aligned}$$

Here we define $H_{dc,i} = \eta_{dc,i} + (1-\beta_c)\psi_{dc,i}$ as given in Eq. (10), which is used for obtaining the optimized D2D-CU matching given in Eq. (9). Similarly, differentiating $\mathcal{L}$ with respect to $P_{dc,i}$ and equating it to zero, we arrive at:

$$\begin{aligned}
&\frac{\partial\mathcal{L}}{\partial P_{dc,i}} = 0 \\
&\frac{-y_{dc,i}g_{dc}(I_{dc}+e_{dc}N_0)}{\ln 2(I_{dc}+f_{dc}P_{dc,i}+e_{dc}N_0)(I_{dc}+(f_{dc}+g_{dc})P_{dc,i}+e_{dc}N_0)} \\
&+\lambda_{d,i}y_{dc,i}+\mu_{d,i}y_{dc,i}\tau_i+\omega_i\,(1-x_c)x_{pc}\frac{\alpha_p}{g_{pc}}y_{dc,i}g^I_{dc} \\
&+\gamma_i x_c\frac{\alpha_c}{g_c}y_{dc,i}g^I_{dc} = 0.
\end{aligned}$$

Considering that the d^{th} D2D link reuses the RB of the c^{th} MU, so that $y_{dc,i} = 1$, we simplify the above equation and

obtain the following equation:

$$s_{dc}^{(0)} P_{dc,i}^2 + s_{dc}^{(1)} P_{dc,i}^2 + s_{dc}^{(2)}(\lambda_{dc,i}, \mu_{dc,i}, \gamma_{dc,i}, \omega_{dc,i}) = 0.$$

This equation is quadratic in $P_{dc,i}$, which is solved to obtain $P_{dc,i}^*$ as given in Eq. (8), where $s_{dc}^{(0)}$, $s_{dc}^{1)}$ and $s_{dc}^{(2)}(\lambda_{dc,i}, \mu_{dc,i}, \gamma_{dc,i}, \omega_{dc,i})$ are defined in Lemma 2.

APPENDIX C

Using Eq. (8) and the constraints of Eq. (5g) and Eq. (5f), we surmise that there exists at least one $P_{dc,i}^* \geq 0$ in the c^{th} RB for any d and c, which satisfies the equation can be derived as shown at the top of the previous page.

For the different combination of $\lambda_{d,i} = 0$ and/or $\mu_{d,i} = 0$ and/or $\gamma_i = 0$ and/or $\omega_i = 0$, we obtain $\lambda_{d,i}^{max}$, $\mu_{d,i}^{max}$, γ_i^{max} and ω_i^{max}.

REFERENCES

[1] F. Malandrino, C. Casetti, and C. F. Chiasserini, "Toward D2D-enhanced heterogeneous networks," *IEEE Commun. Mag.*, vol. 52, no. 11, pp. 94–100, Nov. 2014.
[2] P. Jänis *et al.*, "Device-to-device communication underlaying cellular communications systems," *Int. J. Commun., Netw. Syst. Sci.*, vol. 2, pp. 169–178, Jun. 2009.
[3] D. Feng, L. Lu, Y. Yuan-Wu, G. Y. Li, G. Feng, and S. Li, "Device-to-device communications underlaying cellular networks," *IEEE Trans. Commun.*, vol. 61, no. 8, pp. 3541–3551, Aug. 2013.
[4] A. Ghosh *et al.*, "Heterogeneous cellular networks: From theory to practice," *IEEE Commun. Mag.*, vol. 50, no. 6, pp. 54–64, Jun. 2012.
[5] H. Sun, M. Wildemeersch, M. Sheng, and T. Q. S. Quek, "D2D enhanced heterogeneous cellular networks with dynamic TDD," *IEEE Trans. Wireless Commun.*, vol. 14, no. 8, pp. 4204–4218, Aug. 2015.
[6] Z. Dai, J. Liu, and C. Wang, "QoS-based device-to-device communication schemes in heterogeneous wireless networks," *IET Commun.*, vol. 9, no. 3, pp. 335–341, 2015.
[7] M. Hasan and E. Hossain, "Distributed resource allocation for relay-aided device-to-device communication under channel uncertainties: A stable matching approach," *IEEE Trans. Commun.*, vol. 63, no. 10, pp. 3882–3897, Oct. 2015.
[8] F. Malandrino, Z. Limani, C. Casetti, and C. F. Chiasserini, "Interference-aware downlink and uplink resource allocation in HetNets with D2D support," *IEEE Trans. Wireless Commun.*, vol. 14, no. 5, pp. 2729–2741, May 2015.
[9] J. A. Paradiso and T. Starner, "Energy scavenging for mobile and wireless electronics," *IEEE Pervasive Comput.*, vol. 4, no. 1, pp. 18–27, Jan./Mar. 2005.
[10] N. B. Mehta and C. R. Murthy, "Energy harvesting wireless communication systems," in *Proc. Nat. Conf. Commun.*, India, Feb. 2014.
[11] J. Yang and S. Ulukus, "Optimal packet scheduling in an energy harvesting communication system," *IEEE Trans. Commun.*, vol. 60, no. 1, pp. 220–230, Jan. 2012.
[12] K. Tutuncuoglu and A. Yener, "Optimum transmission policies for battery limited energy harvesting nodes," *IEEE Trans. Wireless Commun.*, vol. 11, no. 3, pp. 1180–1189, Mar. 2012.
[13] P. He, L. Zhao, S. Zhou, and Z. Niu, "Recursive waterfilling for wireless links with energy harvesting transmitters," *IEEE Trans. Veh. Technol.*, vol. 63, no. 3, pp. 1232–1241, Mar. 2014.
[14] B. Medepally and N. B. Mehta, "Voluntary energy harvesting relays and selection in cooperative wireless networks," *IEEE Trans. Wireless Commun.*, vol. 9, no. 11, pp. 3543–3553, Nov. 2010.
[15] I. Ahmed, A. Ikhlef, R. Schober, and R. K. Mallik, "Power allocation for conventional and buffer-aided link adaptive relaying systems with energy harvesting nodes," *IEEE Trans. Wireless Commun.*, vol. 13, no. 3, pp. 1182–1195, Mar. 2014.
[16] S. Gupta, R. Zhang, and L. Hanzo, "Throughput maximization for a buffer-aided successive relaying network employing energy harvesting," *IEEE Trans. Veh. Technol.*, vol. 65, no. 8, pp. 6758–6765, Aug. 2016.
[17] K. Tutuncuoglu, B. Varan, and A. Yener, "Throughput maximization for two-way relay channels with energy harvesting nodes: The impact of relaying strategies," *IEEE Trans. Commun.*, vol. 63, no. 6, pp. 2081–2093, Jun. 2015.
[18] Z. Ding, S. M. Perlaza, I. Esnaola, and H. V. Poor, "Power allocation strategies in energy harvesting wireless cooperative networks," *IEEE Trans. Wireless Commun.*, vol. 13, no. 2, pp. 846–860, Feb. 2014.
[19] N. Roseveare and B. Natarajan, "An alternative perspective on utility maximization in energy-harvesting wireless sensor networks," *IEEE Trans. Veh. Technol.*, vol. 63, no. 1, pp. 344–356, Jan. 2014.
[20] Y. Zhu, L. Wang, K.-K. Wong, S. Jin, and Z. Zheng, "Wireless power transfer in massive MIMO-aided HetNets with user association," *IEEE Trans. Commun.*, vol. 64, no. 10, pp. 4181–4195, Oct. 2016.
[21] D. Liu, Y. Chen, K. K. Chai, T. Zhang, and M. Elkashlan, "Two-dimensional optimization on user association and green energy allocation for HetNets with hybrid energy sources," *IEEE Trans. Commun.*, vol. 63, no. 11, pp. 4111–4124, Nov. 2015.
[22] A. Ghazanfari, H. Tabassum, and E. Hossain, "Ambient RF energy harvesting in ultra-dense small cell networks: Performance and trade-offs," *IEEE Wireless Commun.*, vol. 23, no. 2, pp. 38–45, Apr. 2016.
[23] K. Tutuncuoglu, B. Varan, and A. Yener, "Optimum transmission policies for energy harvesting two-way relay channels," in *Proc. IEEE Int. Conf. Commun. Workshops (ICC)*, Jun. 2013, pp. 586–590.
[24] H. H. Yang, J. Lee, and T. Q. S. Quek, "Heterogeneous cellular network with energy harvesting-based D2D communication," *IEEE Trans. Wireless Commun.*, vol. 15, no. 2, pp. 1406–1419, Feb. 2016.
[25] A. Memmi, Z. Rezki, and M.-S. Alouini, "Power control for D2D underlay cellular networks with channel uncertainty," *IEEE Trans. Wireless Commun.*, vol. 16, no. 2, pp. 1330–1343, Feb. 2017.
[26] P. Sun, K. G. Shin, H. Zhang, and L. He, "Transmit power control for D2D-underlaid cellular networks based on statistical features," *IEEE Trans. Veh. Technol.*, vol. 66, no. 5, pp. 4110–4119, May 2017.
[27] Y. Luo, P. Hong, R. Su, and K. Xue, "Resource allocation for energy harvesting-powered D2D communication underlaying cellular networks," *IEEE Trans. Veh. Technol.*, vol. 66, no. 11, pp. 10486–10498, Nov. 2017.
[28] A. Ramezani-Kebrya, M. Dong, B. Liang, G. Boudreau, and S. H. Seyedmehdi, "Joint power optimization for device-to-device communication in cellular networks with interference control," *IEEE Trans. Wireless Commun.*, vol. 16, no. 8, pp. 5131–5146, Aug. 2017.
[29] D. Fooladivanda and C. Rosenberg, "Joint resource allocation and user association for heterogeneous wireless cellular networks," *IEEE Trans. Wireless Commun.*, vol. 12, no. 1, pp. 248–257, Jan. 2013.
[30] D. Zhu, J. Wang, A. L. Swindlehurst, and C. Zhao, "Downlink resource reuse for device-to-device communications underlaying cellular networks," *IEEE Signal Process. Lett.*, vol. 21, no. 5, pp. 531–534, May 2014.
[31] S. Gupta, S. Kumar, R. Zhang, S. Kalyani, K. Giridhar, and L. Hanzo, "Resource allocation for D2D Links in the FFR and SFR aided cellular downlink," *IEEE Trans. Commun.*, vol. 64, no. 10, pp. 4434–4448, Oct. 2016.
[32] S. Boyd and L. Vandenberghe, *Convex Optimization*. New York, NY, USA: Cambridge Univ. Press, 2004.
[33] C. J. Zarowski, *An Introduction to Numerical Analysis for Electrical and Computer Engineers*. Hoboken, NJ, USA: Wiley, 2004.
[34] E. Suli and D. Mayers, *An Introduction to Numerical Analysis*. Cambridge, U.K.: Cambridge Univ. Press, 2003.
[35] R. Zhang, X. Cheng, L. Yang, and B. Jiao, "Interference graph-based resource allocation (InGRA) for D2D communications underlaying cellular networks," *IEEE Trans. Veh. Technol.*, vol. 64, no. 8, pp. 3844–3850, Aug. 2015.
[36] C. Liu and B. Natarajan, "Power-aware maximization of ergodic capacity in D2D underlay networks," *IEEE Trans. Veh. Technol.*, vol. 66, no. 3, pp. 2727–2739, Mar. 2017.

SHRUTI GUPTA received the B.Tech degree (Hons.) in electronics and communication engineering from the LNM Institute of Information Technology, Jaipur, India, in 2012, and the M.Sc. degree in wireless communications from the University of Southampton, U.K., in 2013, where she is currently pursuing the Ph.D. degree with the Southampton Wireless Group, School of Electronics and Computer Science. Her research interests include energy harvesting, device-to-device communication, cooperative communications, and convex optimization.

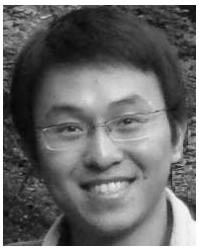

RONG ZHANG (M'09) received the B.Sc. degree from Southeast University, China, in 2003, and the Ph.D. degree from the University of Southampton, U.K., in 2009. He was an Engineer with China Telecom from 2003 to 2004 and also a Research Assistant with the Mobile Virtual Center of Excellence, U.K., from 2006 to 2009. He was a Post-Doctoral Researcher with the University of Southampton from 2009 to 2012. He took an industrial consulting leave from 2012 to 2013 for Huawei Sweden R&D as a System Algorithms Specialist. Since 2013, he has been an Assistant Professor with the Southampton Wireless Group of ECS, University of Southampton. He is also a Visiting Researcher under the Worldwide University Network. He has authored over 40 journals in prestigious publication avenues (e.g., the IEEE and OSA) and many more in major conference proceedings. He was a recipient of joint funding from MVCE and EPSRC. He serves as a reviewer for the IEEE transactions/journals and has served several times as a TPC member/invited session chair of major conferences.

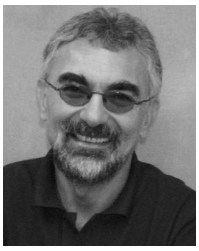

LAJOS HANZO (M'91–SM'92–F'04) received the FIEEE, FIET, D.Sc. degree in electronics in 1976 and the doctorate in 1983. During his 40-year career in telecommunications he has held various research and academic posts in Hungary, Germany, and U.K. Since 1986, he has been with the School of Electronics and Computer Science, University of Southampton, U.K., where he currently holds the Chair in telecommunications. In 2016, he was admitted to the Hungarian Academy of Science. He has successfully supervised 100 Ph.D. students. He is also directing a 60-strong academic research team, involved in a range of research projects in the field of wireless multimedia communications sponsored by industry, the Engineering and Physical Sciences Research Council, U.K., the European Research Council's Advanced Fellow Grant, and the Royal Society's Wolfson Research Merit Award. He is an enthusiastic supporter of industrial and academic liaison and he offers a range of industrial courses. He has co-authored 20 John Wiley/IEEE Press books on mobile radio communications totaling in excess of 10 000 pages, published over 1600 research entries at the IEEE Xplore. He was an FREng, FIET, and a fellow of EURASIP. In 2009, he received the Honorary Doctorate by the Technical University of Budapest and in 2015 by The University of Edinburgh. He has over 25 000 citations and an H-index of 60. He served as the TPC chair and the general chair for the IEEE conferences, presented keynote lectures, and has been received a number of distinctions. He is a Governor of the IEEE VTS. From 2008 to 2012, he was the Editor-in-Chief of the IEEE Press and a Chaired Professor with Tsinghua University, Beijing.